Sediment dispersal in the northwestern Adriatic Sea

Courtney K. Harris,[1] Christopher R. Sherwood,[2] Richard P. Signell,[2]
Aaron J. Bever,[1] and John C. Warner[2]

Received 7 August 2006; revised 14 May 2008; accepted 4 August 2008; published 29 October 2008.

[1] Sediment dispersal in the Adriatic Sea was evaluated using coupled three-dimensional circulation and sediment transport models, representing conditions from autumn 2002 through spring 2003. The calculations accounted for fluvial sources, resuspension by waves and currents, and suspended transport. Sediment fluxes peaked during southwestward Bora wind conditions that produced energetic waves and strengthened the Western Adriatic Coastal Current. Transport along the western Adriatic continental shelf was nearly always to the south, except during brief periods when northward Sirocco winds reduced the coastal current. Much of the modeled fluvial sediment deposition was near river mouths, such as the Po subaqueous delta. Nearly all Po sediment remained in the northern Adriatic. Material from rivers that drain the Apennine Mountains traveled farther before deposition than Po sediment, because it was modeled with a lower settling velocity. Fluvial sediment delivered to areas with high average bed shear stress was more highly dispersed than material delivered to more quiescent areas. Modeled depositional patterns were similar to observed patterns that have developed over longer timescales. Specifically, modeled Po sediment accumulation was thickest near the river mouth with a very thin deposit extending to the northeast, consistent with patterns of modern sediment texture in the northern Adriatic. Sediment resuspended from the bed and delivered by Apennine Rivers was preferentially deposited on the northern side of the Gargano Peninsula, in the location of thick Holocene accumulation. Deposition here was highest during Bora winds when convergences in current velocities and off-shelf flux enhanced delivery of material to the midshelf.

Citation: Harris, C. K., C. R. Sherwood, R. P. Signell, A. J. Bever, and J. C. Warner (2008), Sediment dispersal in the northwestern Adriatic Sea, *J. Geophys. Res.*, *113*, C11S03, doi:10.1029/2006JC003868.

1. Background

[2] The Adriatic is an epicontinental sea that is about 800 km long and 150 km wide (Figure 1). Exchange with the Mediterranean Sea takes place through the Strait of Otranto. The northern Adriatic is shallow (<100 m) and has a very gentle slope ($\sim$0.02°). Depressions that are about 250 m and 1200 m deep, respectively, occupy the middle and southern regions of the Adriatic, and two large cyclonic gyres are often present there [*Artegiani et al.*, 1997; *Poulain*, 2001]. An intensified western boundary current, the Western Adriatic Coastal Current (WACC), flows southward with long-term average speeds that reach 0.20 m s^{-1} at some locations [*Poulain*, 2001].

[3] Two distinct wind regimes, Boras and Siroccos, influence basin-wide circulation in the Adriatic. Boras are cold, dry northeasterly winds while Siroccos are warm, moist southeasterly winds. Bora winds typically intensify the WACC and cause a plume of freshwater and suspended sediment to extend from the Po River region past the Gargano Peninsula [*Orlic et al.*, 1994]. They may also produce a counterclockwise gyre in the northern third of the Adriatic that transports freshwater from the Po River toward the northeast [*Mauri and Poulain*, 2001; *Orlic et al.*, 1994]. Sirocco winds may reduce, or even reverse, the WACC, and confine discharge from northern Adriatic rivers, such as the Po and Adige, to the north [*Orlic et al.*, 1994; *Zavatarelli and Pinardi*, 2003].

[4] Both Bora and Sirocco winds generate energetic waves in the western Adriatic, particularly near the Po Delta (Figure 2). Sirocco winds are aligned with the long axis of the Adriatic Sea, with a nearly unlimited fetch, and therefore generate waves that exert large bed shear stresses in the shallow northern Adriatic. Bora winds have a shorter fetch than Sirocco, but are strong enough to create waves capable of suspending sediment, especially along the northwestern coast [*Fain et al.*, 2007; *Traykovski et al.*, 2007; *Wang et al.*, 2007]. Numerical modeling by *Wang and Pinardi* [2002] concluded that the longer-period waves generated by Sirocco winds were more capable of suspending sediment and created the potential for higher fluxes than waves associated with Bora winds. When the wind-driven currents associated with the waves were included, however, their model estimated higher fluxes under Bora than Sirocco winds [*Wang and Pinardi*, 2002]. Observed fluxes at the Po

[1] Virginia Institute of Marine Science, Gloucester Point, Virginia, USA.
[2] U.S. Geological Survey, Woods Hole, Massachusetts, USA.

0148-0227/08/2006JC003868

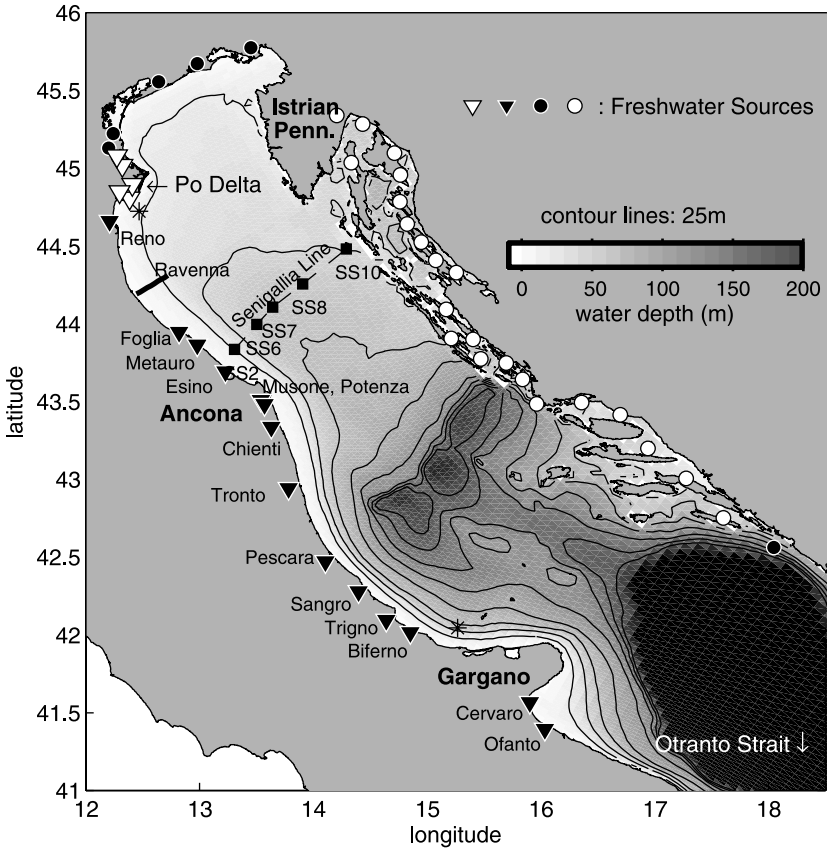

Figure 1. The Adriatic Sea study domain, showing bathymetric contours at 25-m intervals. Depths greater than 200 m not contoured. Triangles identify approximate locations of fluvial sediment sources in model (see Table 1). Po sources are shown as white, and Apennine sources are shown as black triangles. Circles located near modeled freshwater sources for which sediment input was neglected. Black circles are point source rivers, and white circles represent groundwater sources distributed along the Croatian coast. Asterisks mark locations of "Po" and "Gargano" waves in Figure 2. Figure 7 presents data from instruments (black squares) deployed along the "Senigallia Line."

Delta and offshore of the Pescara River showed Bora winds to be important for transport at both locations, while Sirocco conditions also caused significant resuspension offshore of the Po [*Fain et al.*, 2007].

[5] Rivers discharging freshwater and suspended sediments to the Adriatic drain three types of terrain. The Croatian coast is dominated by karst topography. Rivers and groundwater there contribute a fairly large amount of freshwater, but this coastline's sediment input to the Adriatic is negligible [*Cattaneo et al.*, 2003]. Northern Adriatic rivers drain Alpine watersheds that have relatively low sediment yields and contribute much of their sediment during spring snowmelt [*Nelson*, 1970]. Rivers on the east coast of Italy drain the more easily erodible Apennine Mountains, and supply sediment to the Adriatic during discharge pulses associated with precipitation [*Nelson*, 1970].

[6] Tributaries draining both Alpine and Apennine mountain areas contribute to the Po River. The Po accounts for almost a third of the total freshwater ($\sim$47.3 km^3 a^{-1}), and at 13–15 million tonnes per year (Mt a^{-1}) is the largest supplier of sediment to the Adriatic [*Cattaneo et al.*, 2003; *Syvitski and Kettner*, 2007]. Though patterns vary from year to year, high discharge typically results from snowmelt during spring, and precipitation in the lower parts of the catchment from large-scale weather patterns. On the basis of a 15-year record (1989–2003), periods of higher than average Po River discharge typically persist for about a month. As an example, the Po flooded for several weeks in November and December 2002 (Figure 3a).

[7] The relatively short, steep Apennine rivers can be classified as small mountainous rivers, identified by *Milliman and Syvitski* [1992] as supplying the majority of sediment to the coastal ocean. While each individual river does not contribute much sediment, as a group, they account for around 32 Mt a^{-1}, or about 60% of the sediment input to the Adriatic [*Cattaneo et al.*, 2003]. Under natural conditions, flood pulses of the Apennine rivers would persist for a few days, and evidence of the flashiness of these systems is illustrated in Figure 3b. The Apennine rivers have been hydraulically engineered, however, and the hydrograph of each river depends on locally determined policies [*Syvitski and Kettner*, 2007]. For example, base flow of the Pescara River seems to be maintained at an unnaturally high level, while the December 2002 high discharge of the Biferno River seems to have been released more slowly following the precipitation (Figure 3b).

[8] Muddy sediments accumulate offshore of the Po River and along the 40 m isobath of the western coastline.

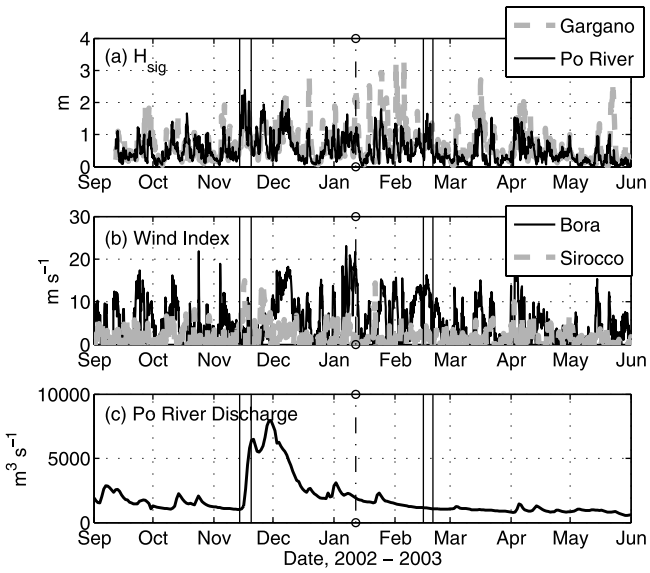

Figure 2. Time series of meteorological forcing for the study period. (a) Waves estimated near Po River and offshore of Gargano Peninsula (see Figure 1). (b) Wind indices (see legend and text). High values indicate Bora or Sirocco conditions. (c) Po River discharge measured at Pontelagoscuro, Italy. Solid vertical lines mark beginning and end of November Sirocco and February Bora shown in Figures 13, 14, 15, and 16. Dashed vertical line marks Bora event that resulted in deposition at Gargano, shown in Figure 18.

Sediment coarsens to sand on either side of the mud belt [*George et al.*, 2007]. Transport seems to bifurcate at the Po Delta, with some material carried southward, and some to the northeast by the northern Adriatic gyre [*Mauri and Poulain*, 2001; *Wang and Pinardi*, 2002]. South of the Po Delta, the WACC carries fine sediment southward [*Wang and Pinardi*, 2002], where some ultimately accumulates as far south as Gargano [*Cattaneo et al.*, 2003; *Frignani et al.*, 2005; *Palinkas and Nittrouer*, 2006]. Various studies have considered the processes that carry sediment from fluvial sources to depocenters along the Apennine margin, but questions remain regarding the degree to which modern, observable sediment transport processes explain depositional patterns [*Cattaneo et al.*, 2003; *Frignani et al.*, 2005; *Palinkas and Nittrouer*, 2006].

[9] Resuspension by waves, transport by currents, and feedbacks between flow and suspended sediment such as bottom boundary layer gravity flows influence continental margin sediment transport [*Grant and Madsen*, 1986; *Smith and Hopkins*, 1972; *Sternberg and Larsen*, 1976; *Traykovski et al.*, 2000]. Bed load is negligible in many coastal environments, except for medium sand and coarser material. Waves dominate resuspension on many continental shelves, including the Adriatic [*Fain et al.*, 2007; *Passega et al.*, 1967; *Puig et al.*, 2007]. On the Po subaqueous delta, downslope gravity flows of near-bed fluid mud can transport sediment distances of about 10 km [*Traykovski et al.*, 2007]. At continental shelf depths away from the delta front, however, gravity flows are less likely to be important because bottom slopes and sediment concentrations in the northern Adriatic are too small to cause significant downslope gravity transport. A sediment budget of the Adriatic concluded that about 10% of the fluvial load may be delivered to the southern Adriatic continental slope and basin [*Frignani et al.*, 2005]. Off-shelf transport of this material appears to be influenced by dense water cascading, and evidence from moorings placed at 600-m water depth show that this is important for sediment transport on the continental slope, particularly within canyons [*Turchetto et al.*, 2007]. At shallower depths, off-shelf transport appears to be driven by the formation of near-bed Ekman spirals where midwater column velocities flow southward parallel to bathymetry as part of the WACC, while near-bed sediment-laden waters flow to the left and offshore. This mechanism has been cited as being important for delivering sediment north of the Gargano Peninsula to water depths of 20–50 m [*Puig et al.*, 2007]. On the basis of these observations, we hypothesize that dilute suspension produced by energetic waves combined with large advection length scales under the WACC dominates dispersal of sediment from fluvial sources to depositional sinks.

2. Objectives

[10] This paper seeks to develop a quantitative understanding of the processes that transport material from source to sink to create geologic signatures. A challenge arises that stems from the gap in temporal and spatial scales inherent in process studies compared to stratigraphic research. Modern process studies evaluate delivery and transport over limited regions for periods of months to a few years [see *Fain et al.*, 2007; *Puig et al.*, 2007; *Traykovski et al.*, 2007; *Turchetto et al.*, 2007]. Stratigraphic studies, on the other hand, provide

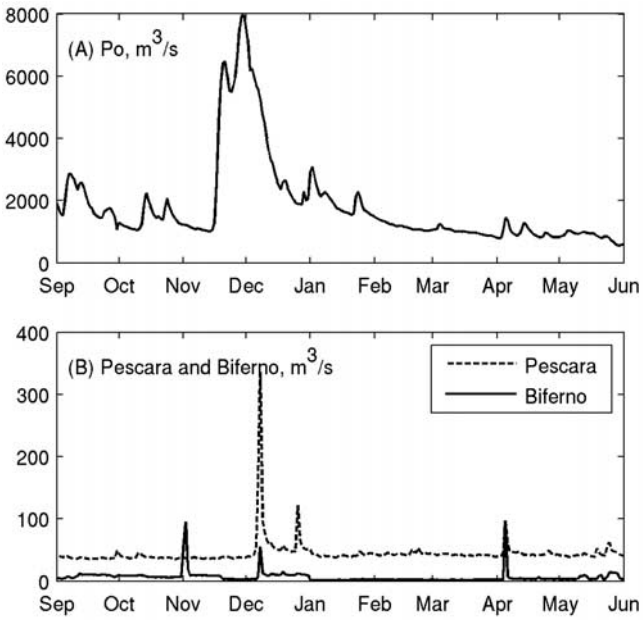

Figure 3. Time series of daily averaged discharge for the (a) Po River, measured at Pontelagascuro, Italy, and the (b) Pescara and Biferno rivers for September 2002 to June 2003. Note factor of 20 difference in scales of Figures 3a and 3b.

information for much longer timescales at spatial scales of geologic units [*Cattaneo et al.*, 2003; *Palinkas and Nittrouer*, 2006, 2007]. With a numerical model we hope to eventually address stratigraphic questions, but preserve the timescales of individual transport events such as storms and floods. We analyze transport and deposition patterns estimated by a coupled hydrodynamic and sediment transport model applied to the Adriatic Sea for a timescale of ten months. While this falls far short of geologic timescales, similarities emerge between modeled deposition and observed stratigraphy. Using the model, we also address the following questions:

[11] 1. What is the short-term fate ($\sim$1 year) of fluvial sediment delivered to the Adriatic?

[12] 2. What are the characteristic temporal and spatial scales of fluvial dispersal in the Adriatic? Is the dispersal dominated by sediment flux during specific meteorological conditions, such as the Bora and Sirocco winds?

[13] 3. To what degree do plume transport, wave and current resuspension, and sediment properties explain the characteristics of observed dispersal in the Adriatic? Do depositional patterns reflect spatial structure in any or all of these?

[14] By analyzing modeled sediment dispersal during this time period, we address the questions stated above and evaluate similarities between Holocene deposition and short-term patterns of dispersal in the Adriatic. Finally, the paper compares spatial patterns in both the waves and currents to evaluate how they contribute to depositional patterns seen in modern and Holocene sediments.

3. Methods

[15] Hydrodynamics, sediment flux, settling, deposition, and erosion were estimated using the Regional Ocean Modeling System (ROMS) for September 2002 to June 2003. Wind and heat flux forcing were derived from COAMPS™ (Coupled Ocean/Atmosphere Mesoscale Prediction System), with spatial and temporal resolutions of 4 km and 3 h [see *Hodur et al.*, 2002; *Pullen et al.*, 2003]. Wavefields were estimated using the SWAN (Shallow Waves Nearshore) model forced by COAMPS input [see *Booij et al.*, 1999; *Ris et al.*, 1999; *Rogers et al.*, 2003; *Signell et al.*, 2005].

[16] ROMS solved the Reynolds-averaged Navier-Stokes (RANS) equation using an s-coordinate vertical grid [see *Shchepetkin and McWilliams*, 2005; *Haidvogel et al.*, 2008]. Twenty vertical layers were stretched to have higher resolution near the water surface and seabed. The model had a horizontal resolution of about 3 km and bathymetry was based on 15 arc second data that included recent multibeam observations from the Consiglio Nazionale delle Ricerche (CNR) [see *Cattaneo et al.*, 2003]. Water depths resolved by the model ranged from a minimum of 4.7 m to a maximum of about 1200 m. A no-gradient condition specified the open boundary for salinity and temperature at the Strait of Otranto. An elevation boundary condition there accounted for tides following *Flather and Proctor* [1983]. Waves influenced flow through wave-current interaction by increasing the bottom drag coefficient [*Madsen*, 1994]. Time steps of 240 s were used.

[17] Initial conditions were interpolated using salinity and temperature data from 239 CTD profiles, most of which were in the northern or western Adriatic. The majority of these were obtained between 16 and 22 September 2002, though conditions in locations deeper than 100 m were collected from 9 to 11 October 2002. Velocity and elevation fields were estimated by running the model for 5 days in diagnostic mode to allow them to adjust to the observed temperature and salinity. The model was then initialized on 16 September 2002 with the resultant temperature, salinity, velocity, and elevation fields.

3.1. Fluvial Sources

[18] Freshwater inflows were specified using a combination of climatological estimates and daily measured data (Table 1). Daily discharge for the Po, Pescara, and Biferno Rivers were used to specify these terms (Figure 3). Three factors complicated attempts to obtain daily values for other freshwater sources. Many of the freshwater sources are not gauged, and data for those that are gauged are maintained locally, not in a centralized data repository. Additionally, because the rivers are hydraulically engineered, daily discharge cannot be easily related to variables such as precipitation [*Syvitski and Kettner*, 2007]. Discharge for groundwater and other rivers were therefore specified using monthly averaged values [*Raicich*, 1996]. Freshwater sources evenly distributed along the eastern coast represented input of Croatian groundwater (white circles in Figure 1).

[19] Measured fluvial sediment discharges were unavailable, though historic data exists for the Apennine and Po Rivers [see *Cattaneo et al.*, 2003; *Frignani et al.*, 2005]. Sediment from rivers to the north and east of the Po contribute little material [*Cattaneo et al.*, 2003] and were neglected (black circles in Figure 1). Sediment input from the Apennine and Po rivers was based on model estimates from HYDROTREND [*Kettner and Syvitski*, 2008; *Syvitski and Kettner*, 2007] that provided rating curves for the Po, Metauro, Pescara, Potenza, and Tronto Rivers. Freshwater and sediment delivery from the Po River was input at points representing the Pila, Tolle, Gnocca, Goro, and Maestra distributaries, on the basis of estimates of the distribution of discharge [*Nelson*, 1970]. For other Apennine rivers the rating curve from the Tronto River was applied, because it seemed characteristic of these rivers. The estimates for Apennine sediment discharge were then adjusted to match the magnitude of delivery cited: 32.2 Mt a^{-1} [*Cattaneo et al.*, 2003].

3.2. Suspended Sediment Calculations

[20] Sediment transport calculations used ROMS sediment routines, described in *Warner et al.* [2008]. Limited to the transport of fine sand, silt and clay, the calculations met the objectives of estimating the dispersal of fluvially delivered material and comparing its transport to that of similarly sized seabed material. Three sources of mobile sediment were included: the seabed, and the Apennine and Po Rivers. Suspended sediment was transported with oceanographic currents, modified by the addition of a prescribed settling velocity. A two-equation turbulence closure submodel using the generic length scale (GLS) method suggested by *Umlauf and Burchard* [2003] represented vertical mixing of water and sediment [*Warner et al.*, 2005]. A no-gradient condition for sediment was applied at the open boundary at the Strait of Otranto. Sediment exchange between the bottommost

Table 1. Fluvial Sources of Freshwater and Sediment Included in the Calculations[a]

Source	Q_{H2O}($m^3 \times 10^{10}$)	Q_{sed}(Mt)	Symbol in Figure 12
Drin[b]	1.05	neglected	
Neretva[b]	1.17	neglected	
Croatia[b]	3.36	neglected	
Isonzo[b]	0.60	neglected	
Tagliamento[b]	0.28	neglected	
Piave[b]	0.16	neglected	
Brenta[b]	0.21	neglected	
Adige[b]	0.69	neglected	
Po[c]	4.38	15.6	
Po Pila	2.67	15.0	large solid circle
Po Tolle	0.53	0.15	large solid circle
Po Gnocca	0.70	0.32	large solid circle
Po Goro	0.35	0.06	large solid circle
Po Maestra	0.13	0.00	large solid circle
All Apennine	0.82	28.9	
Reno[b]	0.15	7.77	open square
Foglia[b]	0.02	0.28	small solid circle
Metauro[d]	0.07	1.73	multiplication sign
Esino[d]	0.08	2.45	addition sign
Musone[d]	0.05	1.01	asterisk
Potenza[d]	0.02	0.29	open diamond
Chienti[b]	0.01	0.05	open rectangle
Tronto[b]	0.12	5.29	open triangle
Pescara[c]	0.16	7.62	solid diamond
Sangro[b]	0.03	0.35	open rectangle
Trigno[b]	0.02	0.29	five-sided star
Biferno[c]	0.03	0.51	six-sided star
Cervaro[b]	0.01	0.07	open circle
Ofanto[b]	0.05	1.22	open rectangle

[a]Left column indicates river name or "Croatia" for input from Croatian groundwater.

[b]Monthly value from *Raicich* [1996].

[c]Measured daily values from Italian Hydrographic Service (personal communication, 2003). Po distributed as 63% Pila, 12% Tolle, 16% Gnocca, 6% Goro, and 3% Maestra following *Nelson* [1970].

[d]Estimate based on yearly average with seasonal trend superimposed, yearly average from *Raicich* [1996].

layer of the water column and the seabed occurred at a rate determined by the difference between sediment settling and upward diffusion, as described below.

[21] The model accounted for six sediment classes, the first being sand resuspended from the bed (type 1) (Table 2). Silt and clay supplied by the bed (type 2) (Table 2) were assigned identical hydrodynamic properties because these seemed to travel as flocculated material, as discussed in section 5.4. Four sediment classes represented material delivered by the Po (types 3 and 4) and Apennine rivers (types 5 and 6) (Table 2). Classes 3 and 5 represented fine grained material that traveled as slow-settling single grains or small aggregates that settled with a velocity (w_s) of 0.01 cm s^{-1}. Flocculated material that settled at 0.1 cm s^{-1} was modeled using types 4 and 6. On the basis of observations by *Fox et al.* [2004], Po sediment was assumed to be 90% flocculated. In contrast, Apennine sediment seemed to consist of less easily flocculated material. For example, lower settling velocities were observed offshore of the Pescara River compared to the Po River [*Mikkelsen et al.*, 2007]. We therefore assumed that 90% of sediment input from the Apennine Rivers settled at 0.1 mm s^{-1}.

[22] Erosion from the seabed was specified following a Partheniades formulation, $E = M f_i (\tau_b/\tau_{cr} - 1)$ where E is an erosion rate (kg m^{-2} s^{-1}), τ_b and τ_{cr} are bed and critical shear stress, respectively, and f_i is the fraction of grain type "i" in the surface active layer (described below). The erosion rate constant, M, was set equal to 5×10^{-5} kg m^{-2} s^{-1}, on the basis of values from the literature [see *Sanford and Maa*, 2001]. Deposition was calculated as the vertical flux of sediment settling from the bottommost layer. Estimates of net erosion and deposition thicknesses were calculated on the basis of the exchange between the seabed and the water column, adjusted for a porosity of 50%. A density of 2650 kg m^{-3} was assumed for sediment. Model calculations of erosion, transport, and accumulation (mass/area) were relatively insensitive to the values chosen for M and porosity, compared to uncertainties in critical shear stresses, sediment settling velocity, and the thickness of the surface active layer.

[23] Limits to the amount available for resuspension via bed consolidation or bed armoring are critical for estimating suspended sediment concentrations [see *Harris and Wiberg*, 2002; *Sanford and Maa*, 2001; *Traykovski et al.*, 2007; *Wiberg et al.*, 1994]. The model limited the amount eroded during a time step to the sediment available in a thin "surface active layer" of the seafloor. The thickness of this layer, usually less than a few millimeters, increased with bed shear stress following *Harris and Wiberg* [2001]. The seabed model tracked grain size characteristics of eight bed layers, the top of which included this surface layer. Each of these bed layers was initially 0.05 m thick, so that the initial sediment bed provided 0.40 m of sediment. While the Partheniades equation is most often applied in cohesive environments, with the inclusion of a surface active layer, it is functionally equivalent to the flux boundary condition applied in noncohesive environments by *Harris and Wiberg* [2001].

3.3. Initial Sediment Distribution

[24] The initial sediment bed was derived by combining grain size observations with a map of sediment texture, limited to fractions of sand, silt, and clay. Grain size data was obtained during 2002–2004 at 205 locations in the Po Delta region and along the Apennine continental shelf by EuroSTRATAFORM colleagues [*George et al.*, 2007; *Palinkas and Nittrouer*, 2006, 2007]. Sediment size fined

Table 2. Sediment Types and Hydrodynamic Properties Used in Numerical

Sediment Source	Sediment Class	Sediment Type	τ_{cr} (Pa)	w_s (mm s^{-1})	Fraction of Input
Seabed	1	sand	0.12	10.0	spatially variable; see Figure 4b
Seabed	2	flocculated fines	0.10	1.0	spatially variable; see Figure 4b
Po River	3	slow settling	0.03	0.1	10% of Po
Po River	4	flocculated	0.08	1.0	90% of Po
Apennine Rivers	5	slow settling	0.03	0.1	90% of Apennine
Apennine Rivers	6	flocculated	0.08	1.0	10% of Apennine

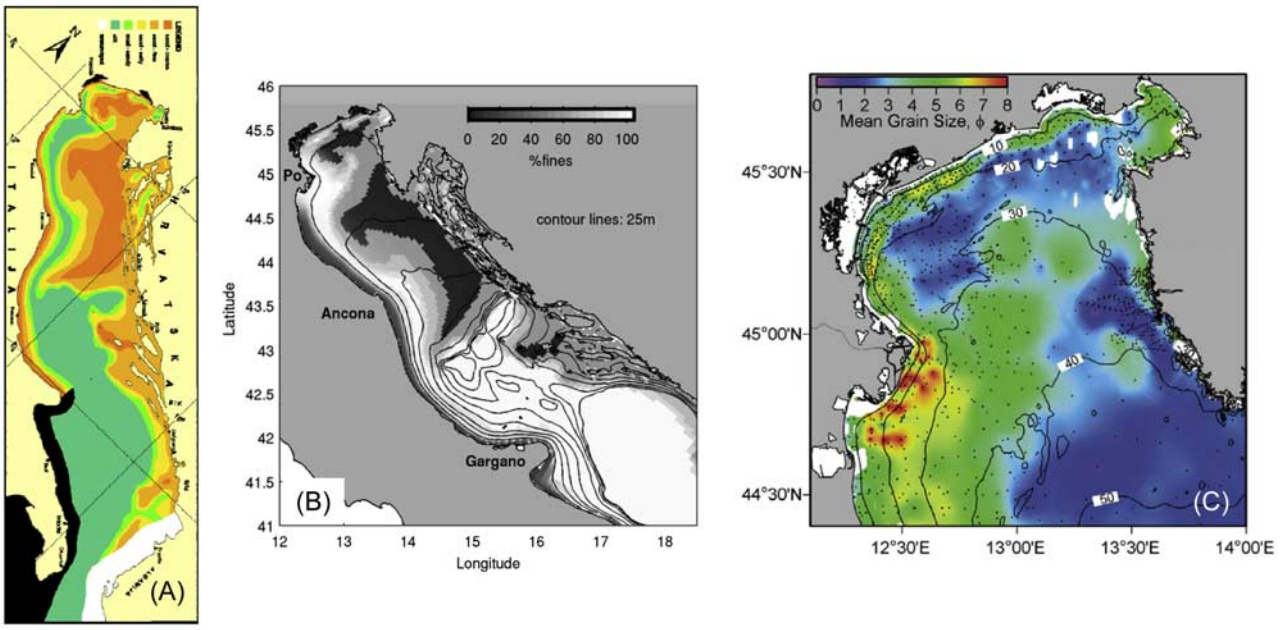

Figure 4. (a) Map of sediment texture taken from historical surveys [*Leder*, 2004]. Fine sediment represented in green, grading to sand in reddish orange. Black and white indicates no data. (b) Initial sediment bed (percent fine) interpolated from historical sediment texture maps combined with recent field observations along the western Adriatic margin as described in text. (c) Sediment texture obtained through geostatistical interpolation by *Goff et al.* [2006].

seaward at these locations. These data were used to derive piecewise linear regressions between sand and silt fraction and water depth for both the Po subaqueous delta and the Apennine margin. Sand, silt, and clay fractions were then assigned to each type of sediment texture shown in the map by *Leder* [2004] (Figure 4a), on the basis of 1181 grain size distributions. For this analysis, the dbSEABED database (C. Jenkins, INSTAAR, personal communication, 2005) provided grain size measurements from *Brambati et al.* [1983] and *Cattaneo et al.* [2003] to supplement EuroSTRATAFORM data. Along the western Adriatic, the initial sediment size distribution was estimated using the

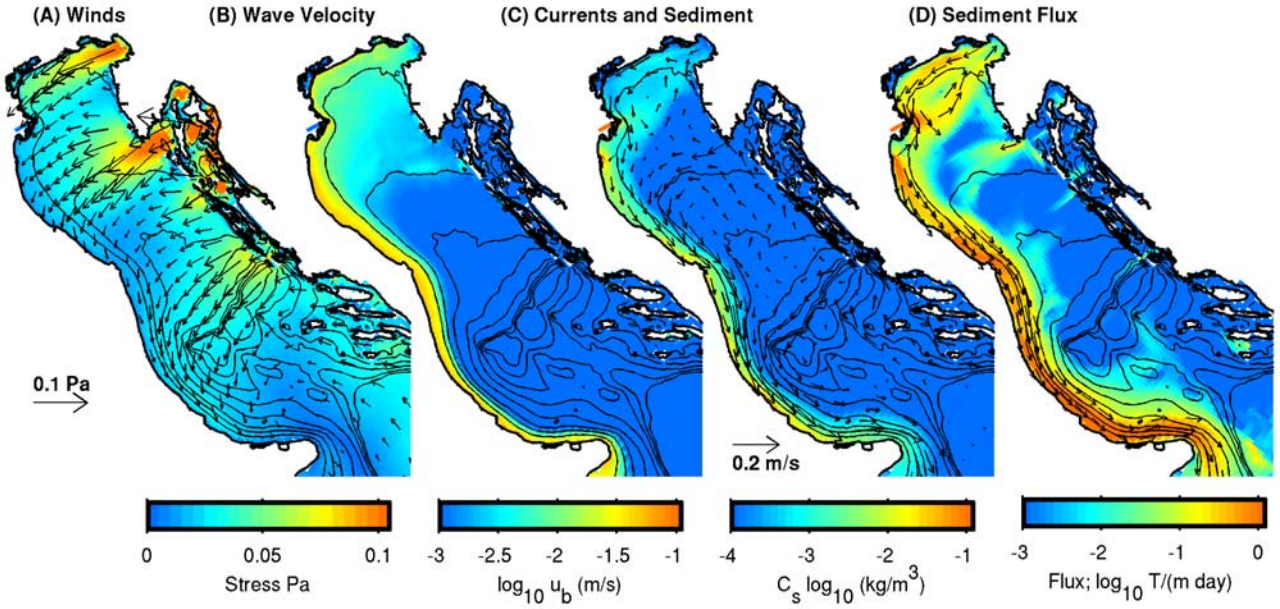

Figure 5. Time-averaged (a) wind stress and (b) wave orbital velocity, (c) depth-averaged suspended sediment concentration (shading) and current velocity (arrows), and (d) depth-integrated daily averaged sediment flux (t m^{-1} d^{-1}). Flux direction shown as arrows where flux exceeds 0.1 t (m d)$^{-1}$. Depth contours at 25 m up to 200-m depth.

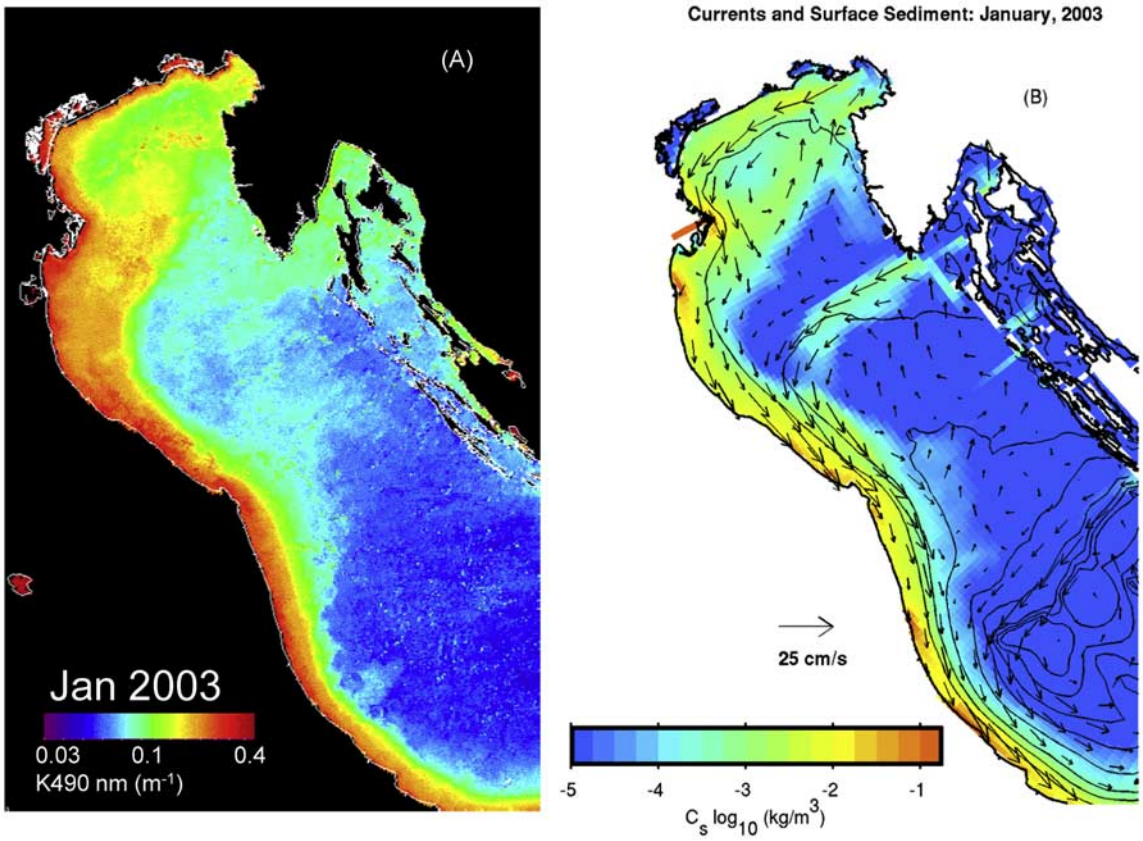

Figure 6. (a) Composite of Moderate Resolution Imaging Spectroradiometer (on EOS) (MODIS) images from January 2003. Extinction coefficient at 490 nm, K490 measured by MODIS on the NASA Aqua polar-orbiting satellite. Analyzed image supplied by E. Mauri, Remote Sensing Group, Istituto Nazionale di Oceanografia e Geofisica Sperimentale, Trieste, Italy. (b) Surface sediment concentration (color) and current velocities (arrows) estimated by the model, averaged for January 2003.

size fraction versus depth relationships obtained for the Po and Apennine shelves. Moving eastward, these were interpolated to values based on the sediment texture map. The resultant estimate of sediment distribution (Figure 4b) contained reliable information on grain size in the western Adriatic, grading to historic information away from the study area. It showed similarities to grain sizes mapped using geostatistical analysis of available data by *Goff et al.* [2006]. Both show fine sediment near the Po Delta, and extending toward the northeast (Figures 4b and 4c).

3.4. Representation of September 2002 to June 2003

[25] Model calculations overlapped the ACE (Adriatic Current Experiment) and EuroSTRATAFORM programs [see *Lee et al.*, 2007; *Nittrouer et al.*, 2004], and contained a significant flood of the Po River, and several Bora and Sirocco wind events (Figure 2). Indices derived from the COAMPS wind velocities indicated the relative strength of Bora and Sirocco conditions (Figure 2b). The Bora index was taken to be the magnitude of the northeast component of the wind velocity offshore of Trieste. The Sirocco wind index was the magnitude of the southeast component of the wind speed, spatially averaged over the portion of the Adriatic that lies north of Ancona. These indicated that Bora conditions occurred frequently and often persisted for several days. Sirocco conditions were evident for only three short times; twice in November, and once in January. To specify discharge of freshwater and sediment, the methods described in section 3.1 were applied to the study period. On the basis of this, the Po River delivered an estimated 15.6 Mt of sediment, and the Apennine rivers delivered an additional 28.9 Mt (Table 1) from September 2002 through June 2003.

4. Results

[26] Results are presented by examining transport, erosion, and deposition of fluvial and bed sediment during the simulation period. Model estimates are compared to observations. Dispersal patterns are then examined in terms of sediment source, the timing of transport, and local signals of transport and deposition.

4.1. Overall Transport Patterns

[27] The modeled sediment transport in the Adriatic was episodic and occurred during storms and floods. Along the Apennine margin, significant flux was calculated during energetic times associated with strong Bora winds, high waves, and a strengthened WACC that typically persisted for 1 day or 2. Near the Po Delta, the largest sediment fluxes were estimated offshore of the Pila distributary during the flood in November and December, and subsequent Bora

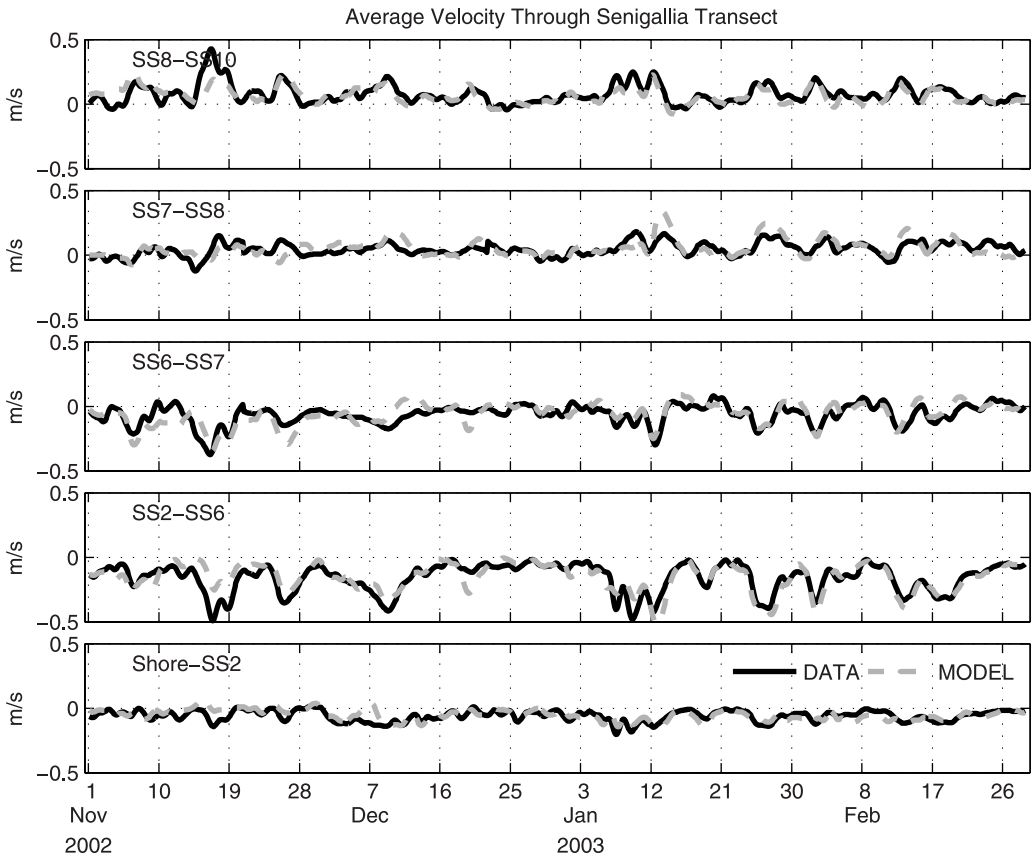

Figure 7. Velocities across Senigallia Line as estimated by Regional Ocean Modeling System and acoustic Doppler current profiler (SS2, SS6, SS8, and SS10) [see *Book et al.*, 2007] and mooring (SS7) measurements. Instrument locations shown in Figure 1, with SS2 and SS10 being the most westward and eastward stations, respectively. SS7 data collected by E. Paschini (CNR-ISMAR, Ancona, unpublished data, 2003) and provided by A. Russo (Università Politecnica delle Marche, personal communication, 2006). Estimates low-pass filtered with a 33 h cutoff frequency. Transports were depth and spatially integrated and then normalized by the mean water depth and across-shelf distance of the transect to give an average velocity (m s^{-1}) for each section. Water depths were 25 m (SS2), 66 m (SS6), 70 m (SS7), 65 m (SS8), and 51 m (SS10).

events. At that site during floods, resuspension and flux peaked during times of energetic waves that were associated with either Bora or Sirocco winds. Other times saw relatively low sediment flux. These findings were consistent with tripod observations of episodic transport in the Adriatic [*Fain et al.*, 2007; *Puig et al.*, 2007; *Traykovski et al.*, 2007].

[28] Time averaged for the ten-month calculations, currents were strongest within the WACC, and the frequent Bora winds strengthened gyres within the northern and central Adriatic (Figure 5). Modeled turbidity was highest offshore of the Po Delta and the coastal zone between Ravenna and Gargano (Figure 5c). Areas of high average sediment concentration did not directly correspond to areas of high average wave orbital velocity (Figures 5b and 5c). The highest sediment flux resulted from advection within the coastal current along the Apennine shelf (Figure 5d). Throughout the time modeled, this transport was to the southeast except for a brief period of northward flow in November, discussed in more detail below. A second transport pathway of sediment followed the gyre in the northern Adriatic formed under Bora winds that carried resuspended sediment and material from the Po River toward the northeast (Figure 5d).

[29] The model reproduced the primary features of northern Adriatic turbidity visible in January 2003 satellite images. A composite of MODIS images indicated that turbid or high-chlorophyll waters were present along the western Adriatic, and in the vicinity of the Po River plume in January 2003 (Figure 6a). Because chlorophyll content is likely low during the winter, this image was compared to model estimates of surface sediment concentration, also averaged for January 2003. Both the model and satellite data indicated the presence of Po River sediment in the southern limb of the counterclockwise northern Adriatic gyre, where model calculations indicated northeastward transport (Figure 6). Also, both showed a widening of the turbid plume offshore of Ancona, and a narrowing of the coastal current to the south.

[30] Comparison of depth and spatially averaged velocities through a transect located offshore of Senigallia (see Figure 1) demonstrated that the model captured both the

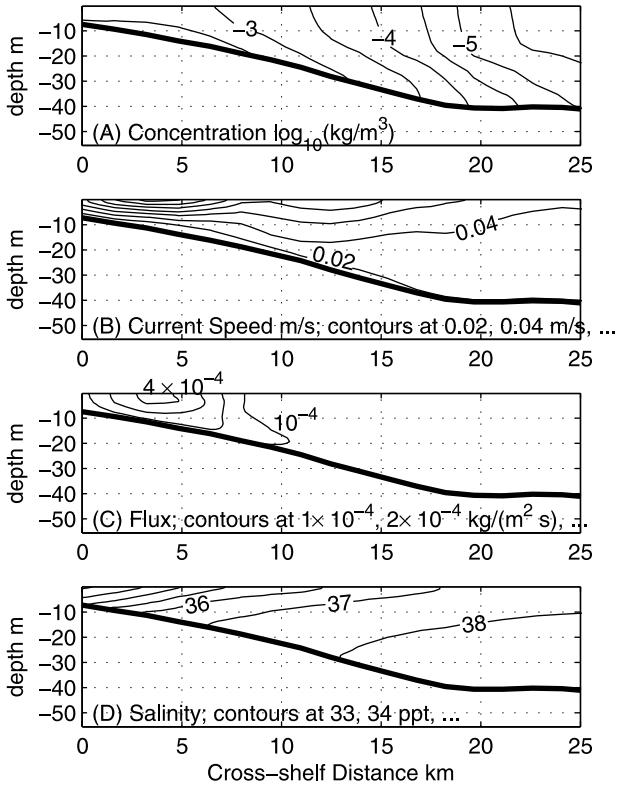

Figure 8. (a) Sediment concentration, (b) current speed, (c) sediment flux, and (d) salinity calculated for the Ravenna transect (location shown in Figure 1), time averaged for the September 2002 to June 2003 calculations.

temporal variability and across-basin structure of flux there (Figure 7). Both data and model estimates showed the overall counterclockwise circulation of the Adriatic, with flux being northward in the eastern Adriatic, and southward in the west. In both the observations and model output, velocities peaked in the portion of the transect between depths of 25 and 66 m (SS2 and SS6). In all sections, flows intensified in response to strong winds. For example, Bora winds on 12 January and from 15 to 20 February 2003 intensified circulation both in the data and the model. Circulation was also seen to be strengthened by a Sirocco on 14–20 November 2002, though the model underestimated the response at this time, especially in the western Adriatic.

[31] At the Ravenna transect western Adriatic sediment concentrations, current velocities, and fluxes were highest inshore of the 20-m isobath (Figure 8). The bottom boundary layer held most of the resuspended sediment (Figure 8a). Flux, however, peaked higher in the water column where currents were faster (Figures 8a, 8b, and 8c). These results were consistent with observations made at this location during February 2003 (W. R. Geyer, personal communication, 2006). Figure 8 illustrates total current speed and sediment fluxes, including both the across-shelf and along-shelf components. Inshore of the 40-m isobath, the along-shelf component dominates with mean along-shelf currents of 0.04–0.06 m s^{-1} and across-shelf currents less than 0.01 m s^{-1}.

4.2. Sediment Dispersal

[32] Net erosion in the western Adriatic accounted for 6.7 Mt of bed material north of the Gargano Peninsula (Table 3), but this estimate was sensitive to the initial sediment bed and its hydrodynamic properties. Overall patterns, however, shed light on resuspension processes. Most of the eroded material was from the fine sediment class (Table 3), which was plentiful and more easily mobilized than the sand class. Fine-grained material was eroded from areas north of the Po Delta, along the 40-m isobath north of Ancona, and the 20-m isobath south of Ancona (Figure 9a). Sand was eroded from areas shallower than 20 m. Erosional patterns seemed to reflect adjustments of the assumed initial sediment bed to hydrodynamic conditions. For example, significant erosion was estimated for the area north of the Po Delta, which was initialized with sediment finer than seen in recent observations (compare Figures 4b and 4c). Estimates of redeposition of bed sediment depended upon modeled areas of flux convergence, and were consistent with observed patterns. Remobilized silt and clay were deposited along the northern edge of the Gargano Peninsula, offshore of Ancona, and the southern side of the Po Delta.

[33] Modeled Po River sediment was confined to the northern Adriatic and only a small fraction was transported toward the Apennine clinoform region (Table 3 and Figure 10a). Most of the sediment delivered by the Po River was deposited close to distributary mouths and was incorporated into a ~1 to 30 cm thick deposit directly offshore of the river, consistent with observations [*Milligan et al.*, 2007; *Palinkas et al.*, 2005]. Po River sediment remained, on average, within 14 km of Po sources, and 92% remained within 20 km of the delta during the ten-month calculations. Much of the Po sediment that traveled further was carried toward the northeast, and contributed to a thin deposit formed underneath the northern Adriatic gyre (Figure 10a) where fine-grained sediments have been observed (Figures 4a, 4b, and 4c). Very little (1%) Po River sediment was transported south of the Foglia River mouth, and only 0.6% traveled as far as Ancona. Nearly all of the Po sediment that was transported southward was characterized with slow settling velocities, but only 10% of this material was transported south of the Reno River mouth.

[34] Most sediment delivered by Apennine rivers was transported toward the southeast (Figure 10b) and traveled further than Po River material, remaining, on average, 28 km

Table 3. Sediment Budget Calculated for September 2002 to June 2003[a]

Source	Sediment Type	Supplied (Mt)	South of Pescara (Mt)
Seabed	overall	6.7	
Seabed	flocculated fines	5.8	
Seabed	sand	0.9	
Po River	overall	15.0	0.02
Po River	flocculated	13.8	0
Po River	slow settling	1.5	0.02
Apennine River	overall	29.0	12.5
Apennine River	flocculated	2.9	0.99
Apennine River	slow settling	26.1	11.5

[a]Includes bed sediment eroded in the western Adriatic to the north of the Gargano Peninsula and fluvial sediment deposited in the western Adriatic.

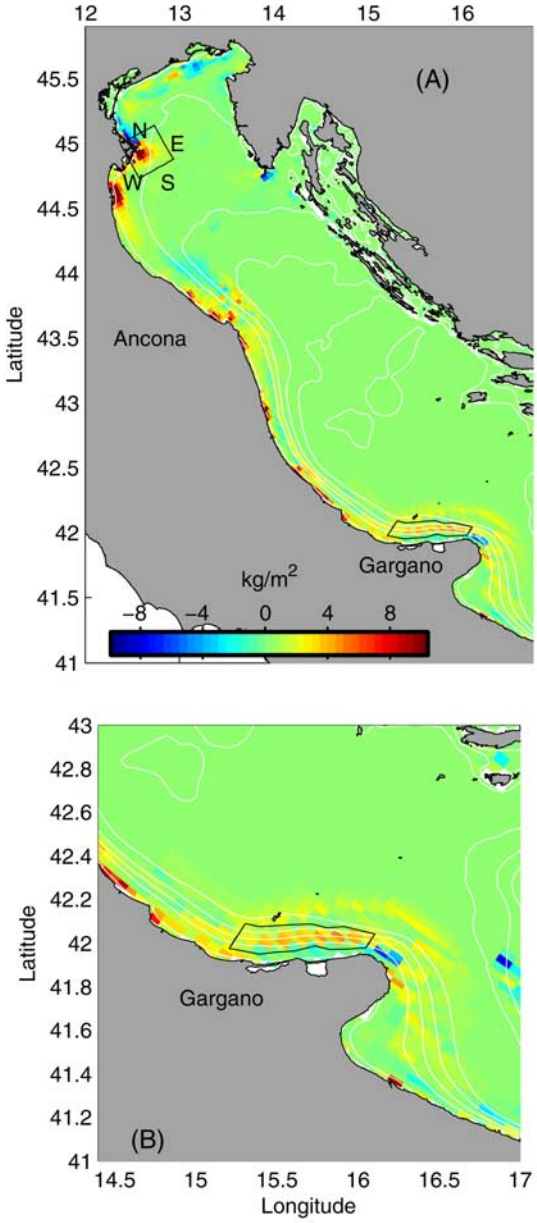

Figure 9. Net erosion (blue) and deposition (red) estimated by model. (a) Entire Adriatic, black boxes show boundaries around deposits at the Po Delta and Gargano Peninsula discussed in text. (b) Enlargement of area near Gargano Peninsula.

from a river source. About 11% of the Apennine load was deposited within 20 km of the Po River mouth; this was mostly material transported northward from the Reno River, which is 25 km south of the Po Delta and supplied about one fourth of the Apennine sediment. This suggests the Reno River supplied much more sediment to the Po Delta region than the Po supplied to the Apennine margin during the study period. Compared to the Po River, Apennine sources dominated sediment supplied to the area south of Pescara (Table 3). At the end of the calculations, 71% of the Apennine sediment was located south of Ancona where it could be incorporated into the Apennine clinoform.

[35] Insights were gained by considering the dispersal of sediment along the axis of the Adriatic (Figure 11). Alongshelf variability in the dispersal of Apennine sediment was apparent. Sediment from most rivers traveled toward the south, except material from the Reno River, which was transported equally to the north and south (Figure 11b). Material from the Po River did not travel very far, but settled close to Po distributary mouths. Though sediment from the Pescara River mixed with material from downstream rivers (the Sangro, Trigno, and Biferno), individual rivers were usually associated with distinct deposits (Figure 11b). Dispersal of sediment away from river sources was quantified using the source/sink ratio, defined as the mass of sediment supplied by the river during the modeled period divided by the mass of fluvial sediment deposited within 10 km of the river mouth (Figure 11c). Large values indicated that the source was much bigger than the deposit, and that sediment was highly dispersed away from that river mouth. If the deposit was larger than the local fluvial source, the source to sink ratio was smaller than one, indicating that sediment from other rivers mixed with material from this source.

[36] Source/sink ratios seemed related to sediment settling velocity, average currents, and bed stress (Figure 12). The large Po-Pila River distributary had a source/sink ratio near 1, indicating that most sediment stayed within 10 km of the river mouth. Because of the higher settling velocity used for Po sediments compared to Apennine sediments, and the fact that bed stresses were lower at the Po Delta, the Po distributaries had a lower source/sink ratio than did many Apennine rivers (Figure 12). Small rivers located downstream from significant sediment sources had source/sink ratios less than one, including the smaller Po distributaries, the Sangro, Trigno, Potenza, and Chienti Rivers. The Pescara River had the second highest source/sink ratio. It empties into an area that experienced both energetic currents and high bed shear stresses (Figure 12). Much of the

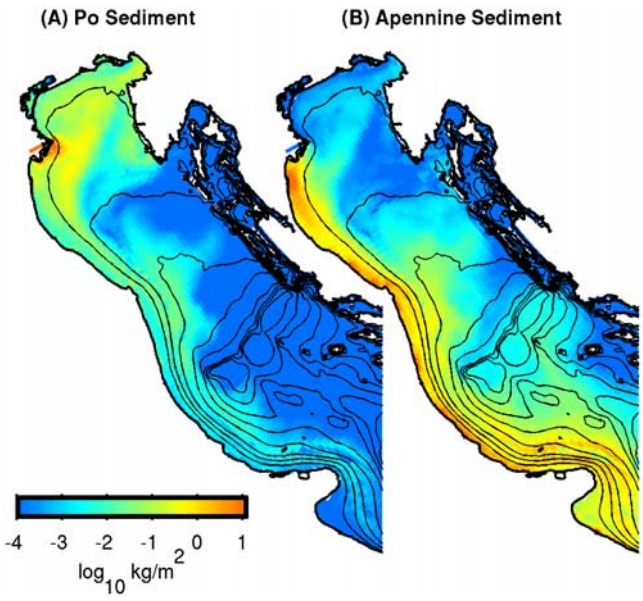

Figure 10. Final deposition of fluvial sediment estimated for the (a) Po River and (b) Apennine rivers. Depth contours at 25 m up to 200-m water depth.

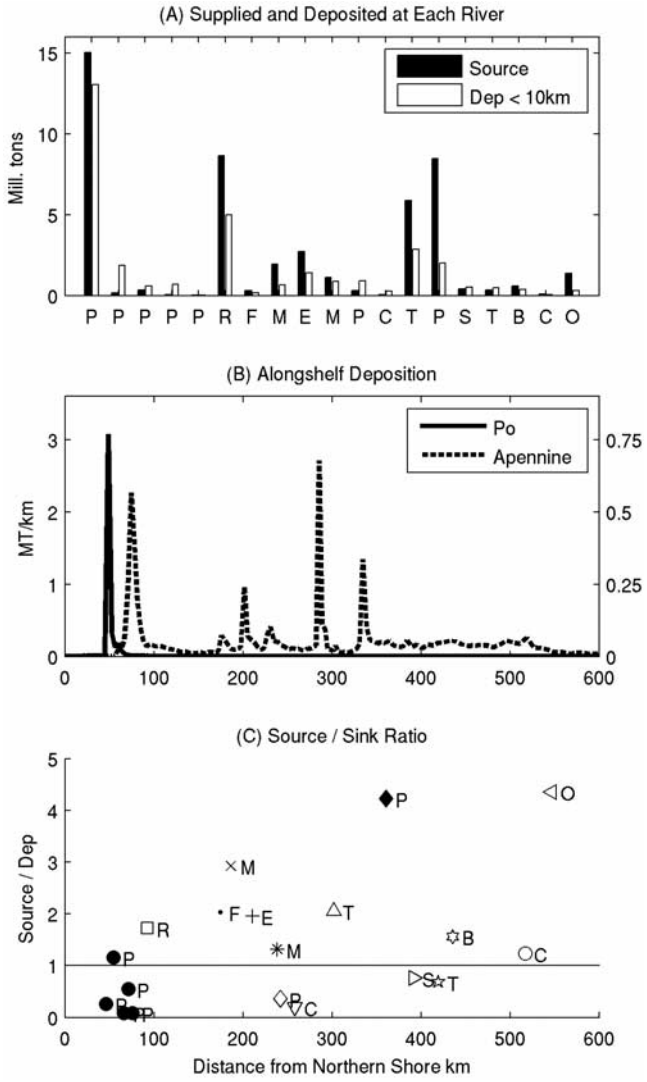

Figure 11. Dispersal of fluvial sediment. (a) Bars show magnitude of fluvial sediment sources and deposition within 10 km of each river mouth. The *x* axis indicates river name (see Table 1). (b) Solid and dashed lines show final distribution of sediment mass from the Po (left *y* axis) and Apennine (right *y* axis) rivers, respectively. The *x* axis is distance from the northern shore. (c) Source/sink ratio between fluvial source of sediment and size of sediment deposit located within 10 km of each river mouth. Rivers identified using first initial of river name and symbols (see Table 1). Each of five Po distributaries shown as a separate bar and point in Figures 11a and 11c.

Pescara River sediment entered during two discharge pulses (Figure 3) that occurred during strong Bora winds, which may have enhanced dispersal. The dispersivity of fluvial systems seemed more related to bed stress than average currents (Figure 12), thus demonstrating the importance of wave resuspension for dispersing sediments.

4.3. Bora and Sirocco Transport

[37] This section characterizes transport patterns for typical Bora and Sirocco conditions using model estimates from comparable events.

[38] From 15 to 20 February 2003, Bora winds created energetic waves in the northern Adriatic and intensified the WACC (Figure 13), as seen in previous studies [*Kourafalou*, 1999; *Wang et al.*, 2007]. The strengthened coastal current transported sediment southward, with flux maximized along the northwestern Adriatic coast and north of the Gargano Peninsula. A gyre also carried material toward the northeast (Figure 13b). Energetic waves and strong currents formed underneath bands of Bora winds to the north and south of the Istrian Peninsula (Figure 13a). The model calculated deposition at the Po Delta, offshore of Ancona and near the Reno River. Dominated by waves, shear stresses peaked in shallow waters along the western Adriatic (Figures 14a and 14b). They were highest between the Po Delta and Ancona, and then decreased, with wave energy, toward Gargano (Figures 14a and 14b). Shear stresses due to currents were, in general, 1 order of magnitude smaller than those generated by waves, and most resuspension occurred in areas of high wave shear stresses.

[39] During Sirocco conditions from 14 to 18 November 2002, winds weakened and even reversed estimated velocities in water depths shallower than 25 m, transporting sediment toward the northwest (Figures 15b and 15c). Currents in deeper water continued to flow southward, including those observed along the Senigallia transect (see Figure 7). While energetic waves were present throughout the Adriatic, many of the western coastal areas were relatively sheltered (Figure 15a). Suspended sediment concentrations peaked at the Po Delta and south of Ancona. Areas of high flux during the Sirocco were smaller and more localized than during the Bora, because the northward winds reduced current velocities (Figures 13c and 15c). The highest sediment fluxes were estimated to be in the region south of Ancona, with northward flux in water depths shallower than 25 m, and southward and offshore flux seaward of this. Shear stresses for this Sirocco period

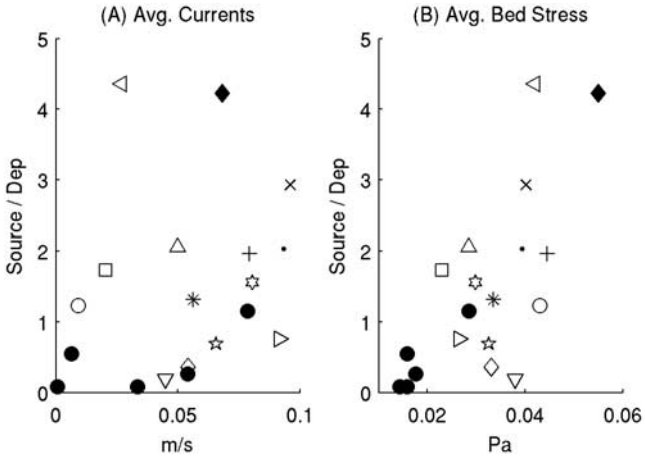

Figure 12. Source/sink ratio of fluvial source to deposit size (*y* axis) compared to (a) time-averaged currents and (b) time-averaged bed shear stress. The *y* axis is the fluvial source divided by the amount of deposition within 10 km of each river mouth. Currents and bed shear stress were time averaged at grid cells within 10 km of each river mouth. Symbols used for each river provided in Table 1.

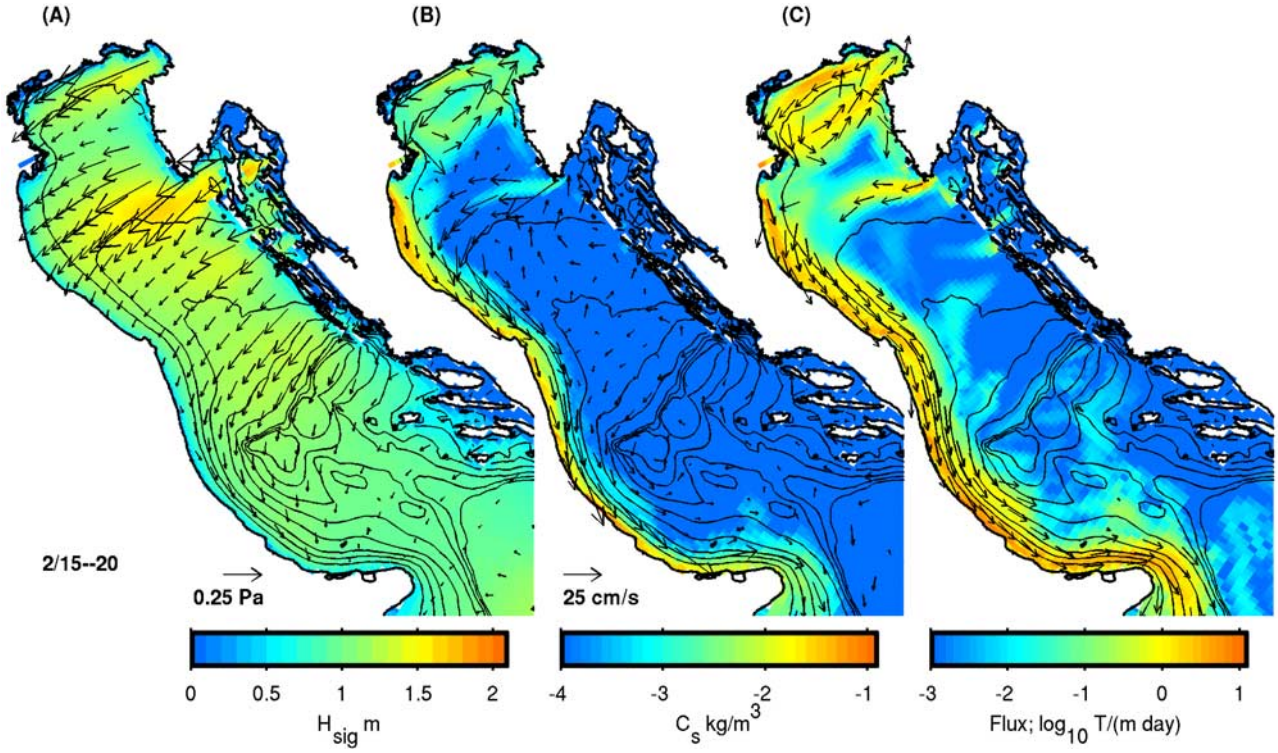

Figure 13. Conditions averaged during a Bora from 15 to 20 February 2003. (a) Wind stress (arrows; see scale for magnitude) and wave height (color). (b) Depth- and time-averaged sediment concentration (color) and current velocity (arrows; see scale for magnitude). (c) Time-averaged, depth-integrated flux (t m^{-1} d^{-1}). Arrows show direction where flux exceeds 0.1 t (m d)$^{-1}$. Contours drawn every 25 m up to 200-m water depth.

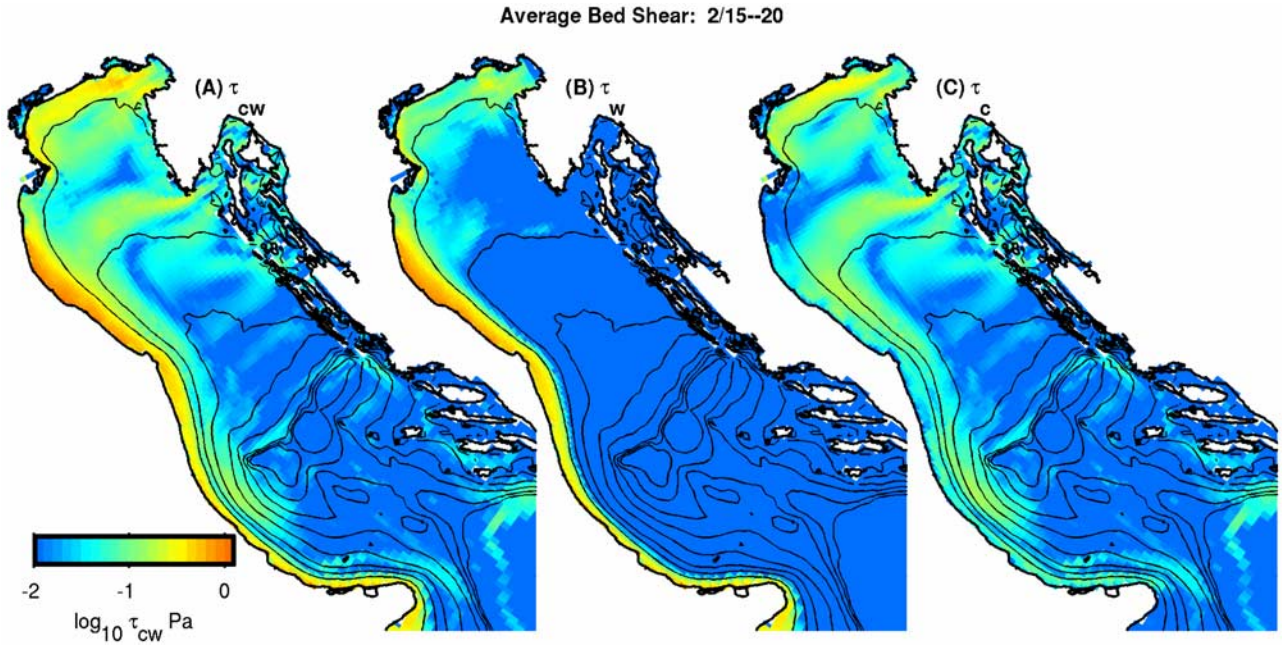

Figure 14. Bed shear stresses averaged during the Bora from 15 to 20 February 2003. (a) Combined wave-current skin friction shear stress. (b) Wave component of shear stress and (c) current component of shear stress. Colors shown in log scale. Contours drawn every 25 m up to 200-m water depth.

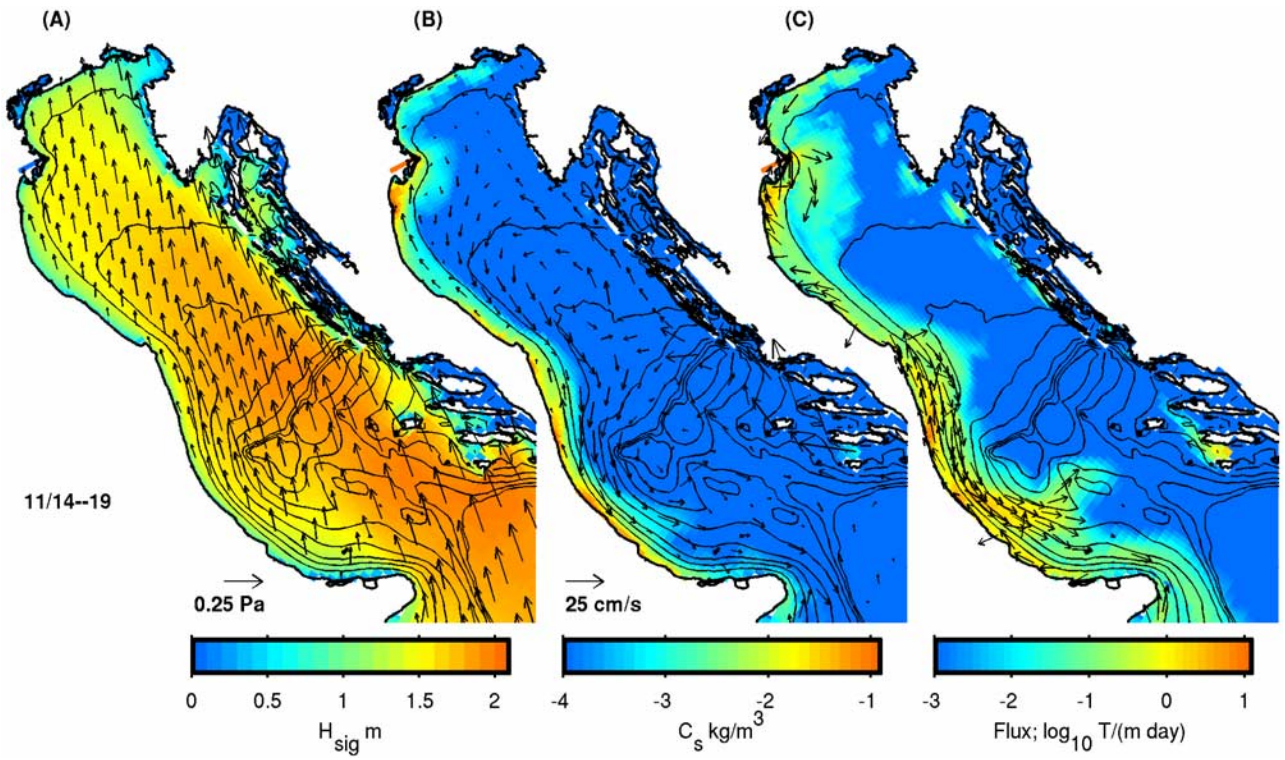

Figure 15. Conditions averaged during a Sirocco, 14–19 November 2002. (a) Wind stress (arrows; see scale) and wave height (color), (b) Depth- and time-averaged sediment concentration (color) and velocity (arrows; see scale). (c) Time-averaged, depth-integrated flux (t m^{-1} d^{-1}). Arrows show direction where flux exceeds 0.1 t (m d)$^{-1}$. Contours every 25 m up to 200-m water depth.

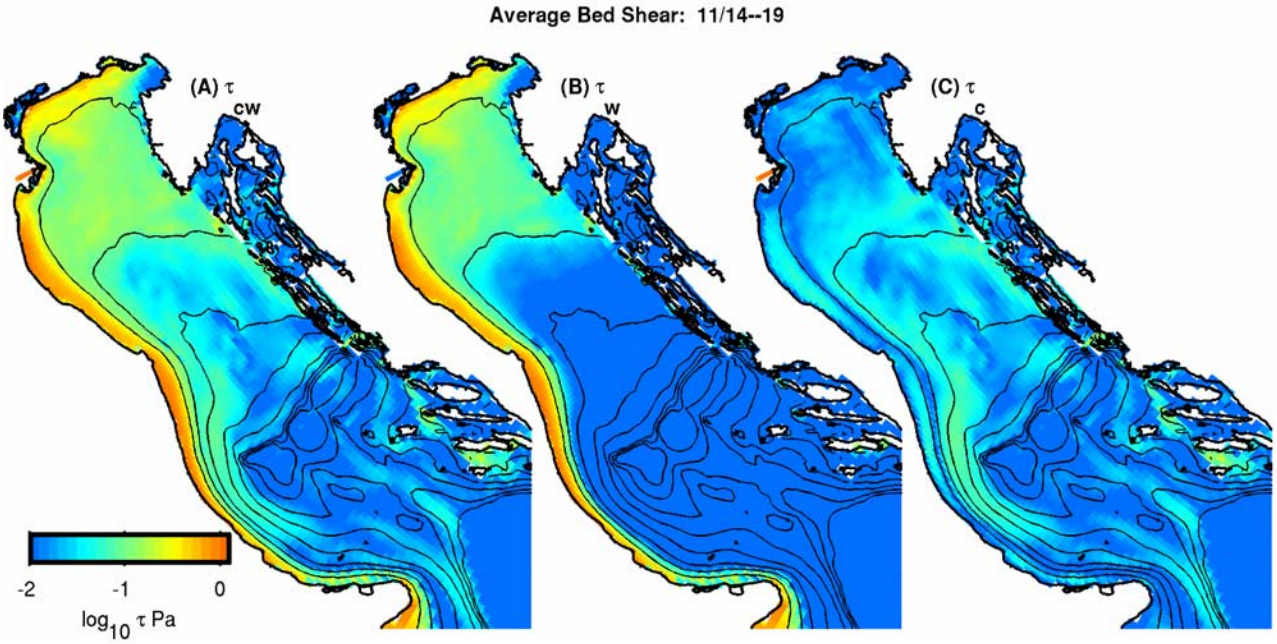

Figure 16. Bed shear stresses averaged during the Sirocco, 14–19 November 2002. (a) Combined wave-current skin friction shear stress, (b) wave component of shear stress, and (c) current component of shear stress. Colors shown in log scale. Contours drawn every 25 m up to 200-m water depth.

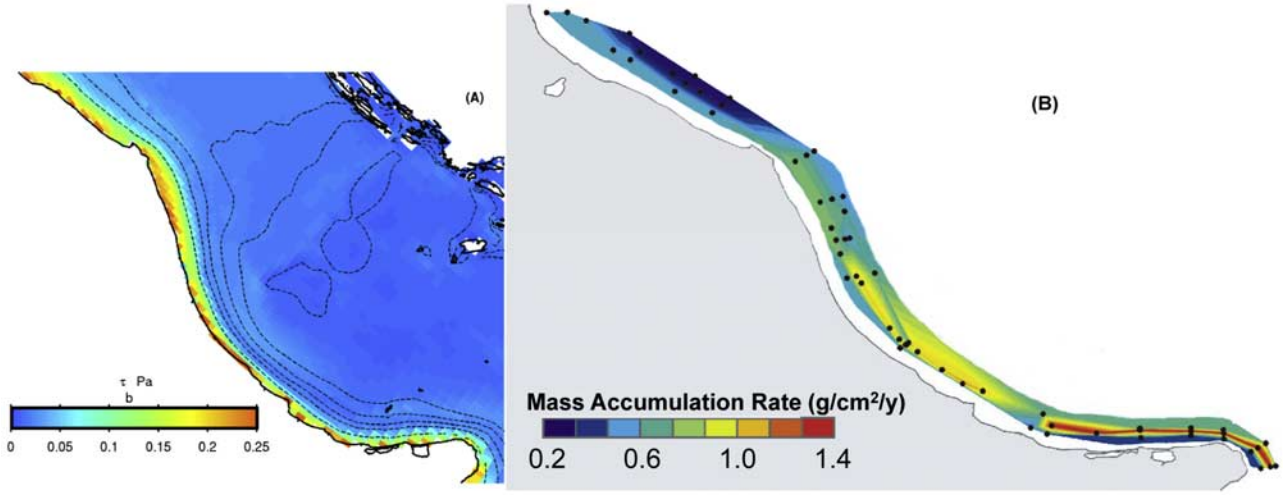

Figure 17. (a) Bed shear stress estimates for the Adriatic, averaged over the 10-month calculations. (b) Accumulation rates estimated using ^{210}Pb, from *Palinkas and Nittrouer* [2006].

peaked in shallow areas of the western coast, but remained high throughout the northern Adriatic (Figure 16a). Indeed, shear stresses for the Sirocco were larger in the northwestern Adriatic than those estimated for the Bora (Figures 14a and 16a). For example, maximum bed shear stresses were 1.4 and 1.0 Pa for these Sirocco and Bora, respectively. Therefore, while the Sirocco produced higher average bed shear stresses and sediment concentrations than the Bora, sediment flux was much lower because Sirocco winds reduced current velocities in the western Adriatic.

4.4. Deposition at the Po Delta and North of the Gargano Peninsula

[40] This section examines factors that contributed to deposition at the Po Delta and north of the Gargano Peninsula, focusing on the areas within boxes on Figure 9.

[41] The Po Delta represents the largest deposit estimated by the model. Flood input dominated deposition at the Po Delta, but this was enhanced by flux convergence. Material delivered directly from the Pila and Tolle mouths of the river accounted for about 10 Mt of sediment, and resuspended bed material during a single Bora in February added about 8% more sediment. Flux converged in the north-to-south direction, in part because of a reduction in southward current velocities. Flux diverged through the eastern and western borders of the control volume. Much more sediment was exported to the east (1.1 Mt) than to the west (0.3 Mt) or south (0.4 Mt).

[42] The Gargano deposit, while much smaller than the Po, was located at a site where accumulation has been observed over longer timescales (see Figure 17b) [*Cattaneo et al.*, 2003; *Palinkas and Nittrouer*, 2006]. Along-shelf flux convergence and across-shelf flux contributed to deposition in the mid-to-outer shelf regions here. Of the 1.4 Mt deposited at Gargano, much (1.1 Mt) was Apennine sediment delivered during the calculations. Resuspended bed sediment accounted for the rest of the deposit. Sediment accumulated here in spite of the fact that, when averaged over the entire simulation, the along-shelf component of current velocity accelerated over the deposit. Seaward flux of inner shelf sediment was likely important, because the model estimated erosion at water depths shallower than 20 m, with deposition seaward of that. Analysis of bed shear stresses show that the area north of the Gargano Peninsula was less impacted by energetic waves and bed stresses than other areas in the western Adriatic (Figure 17a). The pattern toward lower bed stresses, and less frequent storm conditions closely mirrors observed accumulation implied from ^{210}Pb (Figure 17b) [*Palinkas and Nittrouer*, 2006]. This implies that sediment accumulation over 100-year timescales may be related to storm patterns evident within a single year.

[43] Because the 11–16 January 2003 Bora deposited more sediment (0.3 Mt) at the Gargano Peninsula than any other event modeled, it was analyzed to illustrate depositional processes at the Gargano Peninsula over short timescales. During this time, strong winds propagated southward from the area of typical Bora influence, and wave heights peaked at Gargano (Figure 2). Accumulation was highest upstream of the Gargano Peninsula where currents slowed and wave energy decreased (Figures 18a, 18b, and 18d). Centered at the site of Holocene accumulation, sediment was deposited between water depths of 20 and 40 m. Over the length of the deposit, currents decelerated, and wave heights were at a local minimum. The offshore deflection of currents transported sediment to the midshelf (Figures 18b and 18c). Therefore, flux convergence from a decrease in the along-shelf currents, reduced wave energies, and seaward directed flux all contributed to the midshelf deposit upstream of the Gargano Peninsula.

5. Discussion

[44] This section discusses the advection length scales estimated for fluvial sediment. Potential problems with the approach are explored, including difficulties in extending the conclusions to longer timescales.

5.1. Dispersal Lengths

[45] Po and Apennine sediment traveled, on average 14 and 28 km, respectively. Differences in these dispersal

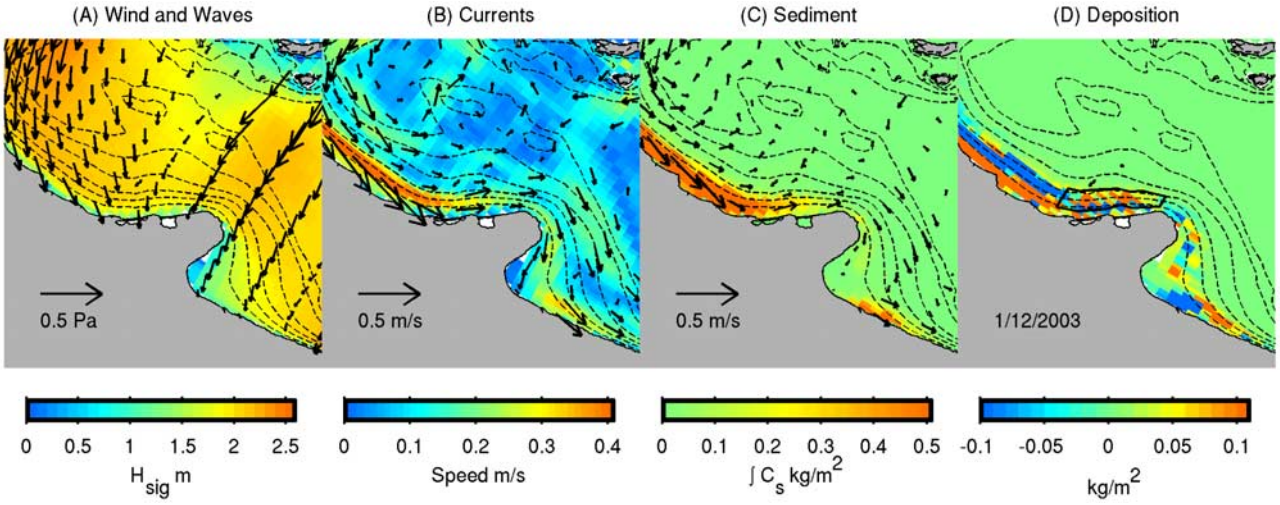

Figure 18. Conditions at the Gargano Peninsula during depositional event on 12 January 2003. (a) Wave height (m, color) and wind stress (arrows), (b) depth-averaged current speed (color) and velocity (arrows) time averaged for 12 January 2003. (c) Sediment concentration time averaged and depth integrated (kg m^{-2}) and currents 1 m above bed (arrows). (d) Deposition (red) and erosion (blue) estimated for that day. Box shows location of "Gargano Deposit" seen in Figure 9. Depth contours drawn every 25 m up to 150-m water depth.

length scales can be explained by the fact that Po River sediment was modeled as entering the Adriatic with a greater fraction of flocculated (fast-settling) material than Apennine sediment (Table 2). In fact, slow-settling material from the Po traveled, on average, further (55 km) than similar material from Apennine rivers (30 km). Flocculated fractions from the Apennine and Po Rivers traveled, on average, 6.1 and 9.6 km, respectively. The timing of sediment supply may explain the shorter distances traveled by Apennine sediment compared to the same material from the Po. One half of the Po sediment reached the coastal ocean by 28 November 2002, while half of the Apennine sediment was delivered by 2 February 2003. Apennine sediment had, on average, 73 fewer days to be transported than Po sediment before the simulation ended.

5.2. Relevance of Seasonal Transport Patterns to Longer Timescales

[46] These calculations were limited to a ten-month study period for which high-resolution winds were available. This prevented direct consideration of how interannual variability, morphodynamics, or extreme events influence dispersal. This section considers interannual variability by placing the study period in the context of longer-term climatic conditions, and then compares estimated transport patterns to observations made over longer timescales.

[47] Discharge from the Po River was slightly higher, and conditions were stormier than normal during the study period. The record of daily discharge of the Po River from Pontelagoscuro, Italy, measured from 1 January 1989 through 3 May 2003, contains fifteen whole or partial water years, defined as October 1 to September 30. Of these, the 2002–2003 water year contained the third highest flood peak at 7960 m^3 s^{-1}. Po River discharge of 3.6×10^{10} m^3 of water from October 2002 to May 2003 ranks fourth for the amount of freshwater delivered during these months in the 15-year record. Both of these metrics indicate that the study period was wetter than normal, though not extremely so. The study period was a time of intense Bora (Figure 2), characteristic of the Adriatic during winter [*Heimann*, 2001]. Analysis of a 5-year record of Quickscat satellite data indicated that this winter period had 40% more Bora, and 11% more Sirocco conditions than average [*Book et al.*, 2007]. The dominance of storm transport of sediment may therefore have been exaggerated in our simulation, simply because Bora and Sirocco conditions occurred more frequently than is typical.

[48] Sediment from the Apennine rivers and resuspended from the bed contributed to the modeled Gargano deposit, but Po River material did not. The model result that nearly all Po sediment remained in the northern Adriatic was insensitive to the settling velocity used. It conflicts, however, with the conclusions of *Palinkas and Nittrouer* [2006], who used measured accumulation rates and budgets of fluvial sediment loads to conclude that the Po River has supplied one half of the sediment to the Gargano deposit. Two explanations exist for the discrepancy between the model result and the interpretation of geochronology. The first explanation is that processes depicted by the model did not represent conditions over the timescale recorded by geochronology, because of interannual or geomorphic variability. Modeled Po River material was trapped by the northern Adriatic gyre, forming deposits in the northern Adriatic that match observations (Figure 6). This trapping may have been particularly effective during our study because it was a time of intense Bora. Also, the configuration of the Po River has been modified and it now occupies a more northerly location than at times in the past [*Correggiari et al.*, 2005; *Nelson*, 1970]. A southward shift of the river mouth could increase dispersal of sediment from the Po River, as discussed by *Bever* [2006]. An alternative explanation is simply that inaccuracies in either accumulation

rates or fluvial sediment loads produce erroneous sediment budgets for the Gargano deposit.

5.3. Challenge of Estimating Sediment Load From the Po River

[49] The Po River drains both Alpine and Apennine watersheds. Apennine areas supply over 6 times higher sediment yields (tons of sediment per area per time) than Alpine regions [see *Cattaneo et al.*, 2003]. The Po River rating curve represents approximately equal contributions to the sediment load from Alpine and Apennine tributaries [*Nelson*, 1970]. In reality, sediment concentration at any given time varies according to whether precipitation was centered over Alpine or Apennine portions of the drainage basin, or whether discharge is fed by snowmelt in the spring or heavy rains in the fall and winter. This produces large scatter in rating curves that estimate sediment concentration as a function of freshwater discharge [*Nelson*, 1970; *Syvitski and Kettner*, 2007]. Rating curve accuracy for rivers such as the Po that include diverse subcatchments might be improved by using different coefficients for each season, but this would require much more data to obtain robust rating curve parameters.

[50] It is unclear, however, whether the available rating curve overestimated or underestimated sediment discharge during the study period. If the rating curve accurately represented the modern Po, it probably underestimated sediment delivery for the November–December 2002 flood, which was likely fed by sediment-rich Apennine tributaries. Precipitation to Alpine regions during this time would have been retained as snow. Some evidence, however, implies that the available rating curve overestimated sediment load. Models applied to the 2002 flood and an earlier one from December 2000 reduced the sediment rating curve reported by *Syvitski and Kettner* [2007] by about one half in order to reproduce flood deposition that compared well to observations [*Bever*, 2006; *Friedrichs and Scully*, 2007]. One explanation for the need to reduce the rating curve is that data used to develop it were obtained several decades ago, before more recent hydraulic controls were enacted [*Friedrichs and Scully*, 2007; *Frignani et al.*, 2005].

5.4. Sensitivity to Hydrodynamic Properties of Sediment

[51] Resuspension calculations were sensitive to the hydrodynamic properties and initial grain size distributions used. Silt and clay make up much of the seabed and fluvially supplied sediment, but specifying their settling velocity and critical shear stress was difficult. Aggregation and disaggregation modifies the settling velocity of mud; and bed consolidation changes its critical shear stresses over small temporal and spatial scales [*Mikkelsen et al.*, 2005; *Toorman*, 1999; *Winterwerp*, 2002]. The model neglected the dynamics of both aggregation and consolidation, but used constant settling velocities and critical shear stresses for each sediment type.

[52] The fluvial material was assumed to contain a mixture of small and large aggregates that settle at 0.1 and 1.0 mm s^{-1}, respectively. This covers the range of values of settling velocities reported by *Mikkelsen et al.* [2007]. Material from the Po River was assumed to be dominantly packaged as large flocs (90%), while material from the Apennine Rivers was assumed to include only 10% large flocs. As discussed earlier, these assumptions influenced the estimates of advection length scales for the two fluvial systems such that, overall, Apennine material traveled further from the source than did Po material. While the actual distance traveled during the time modeled was sensitive to assumptions about settling velocity, overall conclusions regarding the dispersal were less so. For example, the conclusion that Po River material remained in the northern Adriatic was true for both the slow-settling (w_s = 0.1 mm s^{-1}) and the large floc size class (w_s = 1.0 mm s^{-1}). Only 1.3% of the slow-settling material traveled south to the Pescara transect (Table 3). Our conclusion that the Po River did not deliver much sediment to the Apennine margin during the study period was insensitive to our assumptions about sediment settling velocity.

[53] Settling velocity and critical shear stress for seafloor mud was chosen to be 0.1 cm s^{-1} and 0.1 Pa, respectively, on the basis of near-bed observations offshore of the Chienti River and consistent with values reported by *Mikkelsen et al.* [2007] and *Stevens et al.* [2007]. These represent flocculated and somewhat consolidated mud. In addition to being consistent with direct observations, these model inputs provided results that compared favorably with hydrographic measurements made in February 2003 that placed maximum southward sediment flux shoreward of the 30-m isobath (Figure 8) (W. R. Geyer, personal communication, 2006). When lower values were used that were consistent with Stoke's settling velocity and Shield's critical shear stress curve for individual particles, modeled peak flux was on the outer shelf instead of near the 20-m isobath.

6. Conclusions

[54] The modeling system used here represented the major processes that control sediment dispersal in the Adriatic: wave-current resuspension and transport by currents. Winds, waves, and currents used to drive sediment resuspension and transport within this model captured subtidal temporal variability and regional spatial patterns (Figures 6 and 7). The model reproduced coastal current structure and flux (Figure 7), and large-scale depositional patterns.

[55] Sediment redistribution within the Adriatic depended on sediment properties including settling velocity and critical shear stress, as well as oceanographic conditions such as current velocity and wave energy. The dispersal of fluvial sediment depended strongly on the fraction of sediment packaged as large, fast-settling flocs, and also on the bed shear stresses found offshore of the river mouth. Over the timescale considered, most deposition occurred near river mouths and formed distinct deposits at most fluvial sources. These deposits were continuous only in areas where local sediment supplies from small rivers were overwhelmed by larger upstream rivers.

[56] Po River sediment, packaged mostly as flocculated material [*Fox et al.*, 2004], settled quickly to the bed upon delivery to the coastal ocean, with high deposition rates estimated at Po River mouths. Po sediment delivered as slower-settling material (w_s = 0.1 mm s^{-1}) was more widely dispersed. Nearly all was retained within the northern Adriatic, however, with some transported toward the north-

east by a gyre that formed under strong Bora winds. A small fraction was transported by the WACC toward the Apennine margin and clinoform.

[57] Apennine sediment, delivered mostly as slowly settling material (w_s = 0.1 mm s^{-1}), traveled further than Po sediment, on average. While deposition was highest near river mouths, transport within the WACC enabled Apennine sediment to contribute significantly to deposition north of the Gargano Peninsula.

[58] In the western Adriatic, Bora conditions tended to maximize sediment flux, because they strengthened both waves and the WACC. While Sirocco conditions produced energetic waves and high suspended sediment concentrations, the northward winds decreased currents and sediment flux.

[59] Convergence caused by deceleration of current velocities at times enhanced accumulation at both the Po Delta and north of the Gargano Peninsula. At the Po Delta, a single flood dominated accumulation. Deposition on the northeast side of the Gargano Peninsula produced a pattern that was intriguingly similar to those seen in Holocene maps for a 100-year timescale [*Cattaneo et al.*, 2003; *Palinkas and Nittrouer*, 2006]. Reduced wave energy, seaward transport during storms, and flux convergence driven by episodic reduction in current velocities seemed to contribute to sediment deposition here.

[60] **Acknowledgments.** The authors are grateful for funding and support from the Office of Naval Research's Coastal Geosciences and Marine Modeling programs, the U.S. Geological Survey, and NATO's SACLANT-CEN. Comments from H.-S. Kim (U.S. Geological Survey), C. Palinkas (UMCES), and two anonymous reviewers greatly improved the paper. Model inputs relied on bathymetric data provided by F. Trincardi (CNR), COAMPS estimates from J. Doyle (Naval Research Laboratory), and grain size data accessed using dbSeabed courtesy of C. Jenkins (Institute for Arctic and Alpine Research). E. Paschini (CNR-ISMAR, Ancona) and A. Russo (Università Politecnica delle Marche) supplied data from the "SS7" mooring used in Figure 7. We also thank J. Goff (UTIG), N. Leder (Hydrographic Institute of the Republic of Croatia), E. Mauri (Istituto Nazionale di Oceanografia e Geofisica Sperimentale), and C. Palinkas (UMCES) for contributing figures to the paper. This is contribution number 2951 from the Virginia Institute of Marine Science.

References

Artegiani, A., E. Paschini, A. Russo, D. Bregant, F. Raicich, and N. Pinardi (1997), The Adriatic Sea general circulation. Part I: Air-sea interactions and water mass structure, *J. Phys. Oceanogr.*, *27*, 1492–1513, doi:10.1175/1520-0485(1997)027<1492:TASGCP>2.0.CO;2.

Bever, A. (2006), Physical processes behind delta propagation and flood layer dynamics: Po River, Italy, M.S. thesis, Coll. of William and Mary, Gloucester Point, Va.

Booij, N., R. C. Ris, and L. H. Holthuijsen (1999), A third-generation wave model for coastal regions 1. Model description and validation, *J. Geophys. Res.*, *104*, 7649–7666, doi:10.1029/98JC02622.

Book, J. W., R. P. Signell, and H. Perkins (2007), Measurements of storm and nonstorm circulation in the northern Adriatic: October 2002 through April 2003, *J. Geophys. Res.*, *112*, C11S92, doi:10.1029/2006JC003556.

Brambati, A., M. Ciabattie, G. P. Fanzutti, F. Marabini, and R. Marocco (1983), A new sedimentological textural map of the northern and central Adriatic Sea, *Bollettino Oceanol. Teor. Appl.*, *1*, 267–271.

Cattaneo, A., A. Correggiari, L. Langone, and F. Trincardi (2003), The late-Holocene Gargano subaqueous delta, Adriatic shelf: Sediment pathways and supply fluctuations, *Mar. Geol.*, *193*, 61–91, doi:10.1016/S0025-3227(02)00614-X.

Correggiari, A., A. Cattaneo, and F. Trincardi (2005), Depositional patterns in the late-Holocene Po Delta system, in River Deltas—Concepts, Models and Examples, edited by L. Giosan and J. P. Bhattacharya, *Spec. Publ. Soc. Econ. Paleontol. Mineral.*, 83, 365–392.

Fain, A., A. Ogston, and R. W. Sternberg (2007), Sediment transport event analysis on the western Adriatic continental shelf, *Cont. Shelf Res.*, *27*, 431–451, doi:10.1016/j.csr.2005.03.007.

Flather, R. A., and R. Proctor (1983), Prediction of North Sea storm surges using numerical models: Recent developments in the U.K, in *North Sea Dynamics*, edited by J. Sundermann and W. Lenz, pp. 299–317, Springer, New York.

Fox, J. M., P. S. Hill, T. G. Milligan, A. S. Ogston, and A. Boldrin (2004), Floc fraction in the waters of the Po River prodelta, *Cont. Shelf Res.*, *24*, 1699–1715, doi:10.1016/j.csr.2004.05.009.

Friedrichs, C. T., and M. E. Scully (2007), Modeling deposition by wave-supported gravity flows on the Po River prodelta: From seasonal floods to prograding clinoforms, *Cont. Shelf Res.*, *27*, 322–337, doi:10.1016/j.csr.2006.11.002.

Frignani, M., L. Langone, M. Ravaioli, D. Sorgente, F. Alvisi, and S. Albertazzi (2005), Fine-sediment mass balance in the western Adriatic continental shelf over a century timescale, *Mar. Geol.*, *222–223*, 113–133, doi:10.1016/j.margeo.2005.06.016.

George, D. A., P. S. Hill, and T. G. Milligan (2007), Flocculation, heavy metals (Cu, Pb, Zn) and the sand-mud transition on the Adriatic continental shelf, Italy, *Cont. Shelf Res.*, *27*, 475–488, doi:10.1016/j.csr.2005.06.013.

Goff, J. A., C. Jenkins, and B. Calder (2006), Maximum a posteriori resampling of noisy, spatially correlated data, *Geochem. Geophys. Geosyst.*, *7*, Q08003, doi:10.1029/2006GC001297.

Grant, W. D., and O. S. Madsen (1986), The continental shelf bottom boundary layer, *Annu. Rev. Fluid Mech.*, *18*, 265–305, doi:10.1146/annurev.fl.18.010186.001405.

Haidvogel, D. B., et al. (2008), Ocean forecasting in terrain-following coordinates: Formulation and skill assessment of the Regional Ocean Modeling System, *J. Comput. Phys.*, *227*, 3595–3624.

Harris, C. K., and P. L. Wiberg (2001), A two-dimensional, time-dependent model of suspended sediment transport and bed reworking for continental shelves, *Comput. Geosci.*, *27*, 675–690, doi:10.1016/S0098-3004(00)00122-9.

Harris, C. K., and P. L. Wiberg (2002), Across-shelf sediment transport: Interactions between suspended sediment and bed sediment, *J. Geophys. Res.*, *107*(C1), 3008, doi:10.1029/2000JC000634.

Heimann, D. (2001), A model-based wind climatology of the eastern Adriatic coast, *Meteorol. Z.*, *10*(1), 5–16, doi:10.1127/0941-2948/2001/0010-0005.

Hodur, R. M., J. Pullen, J. Cummings, X. Hong, J. D. Doyle, P. Martin, and M. A. Rennick (2002), The Coupled Ocean/Atmosphere Mesoscale Prediction System (COAMPS), *Oceanogr. (Wash. D.C.)*, *15*, 88–98.

Kettner, A. J., and J. P. M. Syvitski (2008), Predicting discharge and sediment flux of the Po River, Italy since the late glacial maximum, in *Analogue and Numerical Forward Modelling of Sedimentary Systems: From Understanding to Prediction*, edited by P. L. de Boer et al., *Spec. Publ. Int. Assoc. Sedimentol.*, *40*, 171–190.

Kourafalou, V. H. (1999), Process studies on the Po River plume, north Adriatic Sea, *J. Geophys. Res.*, *104*, 29,963–29,985, doi:10.1029/1999JC900217.

Leder, N. (Ed.) (2004), Adriatic Sea Pilot, part B-1, pilot, pp. 19–37, Hydrogr. Inst. of the Repub. of Croatia, Split, Croatia.

Lee, C. M., M. Orlic, P. Poulain, and B. Cushman-Roisin (2007), Introduction to special section: Recent advances in oceanography and marine meteorology of the Adriatic Sea, *J. Geophys. Res.*, *112*, C03S01, doi:10.1029/2007JC004115.

Madsen, O. S. (1994), Spectral wave-current bottom boundary layer flows, paper presented at 24th International Conference, Coastal Eng. Res. Counc., Kobe, Japan, 23–28 Oct.

Mauri, E., and P.-M. Poulain (2001), Northern Adriatic Sea surface circulation and temperature/pigment fields in September and October 1997, *J. Mar. Syst.*, *29*(1–4), 51–67, doi:10.1016/S0924-7963(01)00009-4.

Mikkelsen, O., T. Milligan, P. Hill, and R. Chant (2005), In situ particle size distributions and volume concentrations from a LISST-100 laser particle sizer and a digital floc camera, *Cont. Shelf Res.*, *25*, 1959–1978, doi:10.1016/j.csr.2005.07.001.

Mikkelsen, O. A., P. S. Hill, and T. G. Milligan (2007), Seasonal and spatial variation of floc size, settling velocity, and density on the inner Adriatic Shelf (Italy), *Cont. Shelf Res.*, *27*, 417–430, doi:10.1016/j.csr.2006.11.004.

Milligan, T. G., P. S. Hill, and A. B. Law (2007), Flocculation and the loss of sediment from the Po River plume, *Cont. Shelf Res.*, *27*, 309–321, doi:10.1016/j.csr.2006.11.008.

Milliman, J. D., and J. P. M. Syvitski (1992), Geomorphic/tectonic control of sediment discharge to the ocean: The importance of small mountainous rivers, *J. Geol.*, *100*, 525–544.

Nelson, B. (1970), Hydrography, sediment dispersal, and recent historical development of the Po River delta, Italy, in *Deltaic Sedimentation Modern and Ancient*, edited by J. P. Morgan and R. H. Shaver, *Spec. Publ. Soc. Econ. Paleontol. Mineral.*, *15*, 152–184.

Nittrouer, C. A., S. Miserocchi, and F. Trincardi (2004), The PASTA Project: Investigation of Po and Apennine Sediment Transport and Accumulation, *Oceanogr. (Wash. D.C.)*, *17*, 46–57.

Orlic, M., M. Kuzmic, and M. Pasaric (1994), Response of the Adriatic Sea to the Bora and Sirocco forcing, *Cont. Shelf Res.*, *14*, 91–116, doi:10.1016/0278-4343(94)90007-8.

Palinkas, C. M., and C. A. Nittrouer (2006), Clinoform sedimentation along the Apennine River shelf, Adriatic Sea, *Mar. Geol.*, *234*, 245–260, doi:10.1016/j.margeo.2006.09.006.

Palinkas, C. M., and C. A. Nittrouer (2007), Modern sediment accumulation on the Po shelf, Adriatic Sea, *Cont. Shelf Res.*, *27*, 489–505, doi:10.1016/j.csr.2006.11.006.

Palinkas, C. M., C. A. Nittrouer, R. A. Wheatcroft, and L. Langone (2005), The use of ^{7}Be to identify event and seasonal sedimentation near the Po River delta, Adriatic Sea, *Mar. Geol.*, *222–223*, 95–112, doi:10.1016/j.margeo.2005.06.011.

Passega, R., A. Rizzini, and G. Borghetti (1967), Transport of sediments by waves, Adriatic coastal shelf, Italy, *Am. Assoc. Pet. Geol. Bull.*, *51*(7), 1304–1319.

Poulain, P.-M. (2001), Adriatic Sea surface circulation as derived from drifter data between 1990 and 1999, *J. Mar. Syst.*, *29*(1–4), 3–32, doi:10.1016/S0924-7963(01)00007-0.

Puig, P., A. S. Ogston, J. Guillen, A. M. V. Fain, and A. Palanques (2007), Sediment transport processes from the topset to the foreset of a crenulated clinoform (Adriatic Sea), *Cont. Shelf Res.*, *27*, 452–474, doi:10.1016/j.csr.2006.11.005.

Pullen, J., J. D. Doyle, R. Hodur, A. Ogston, J. W. Book, H. Perkins, and R. Signell (2003), Coupled ocean-atmosphere nested modeling of the Adriatic Sea during winter and spring 2001, *J. Geophys. Res.*, *108*(C10), 3320, doi:10.1029/2003JC001780.

Raicich, F. (1996), On the fresh water balance of the Adriatic Sea, *J. Mar. Syst.*, *9*(3–4), 305–319, doi:10.1016/S0924-7963(96)00042-5.

Ris, R. C., L. H. Holthuijsen, and N. Booij (1999), A third-generation wave model for coastal regions. 2. Verification, *J. Geophys. Res.*, *104*, 7667–7681, doi:10.1029/1998JC900123.

Rogers, W. E., P. A. Hwang, and D. W. Wang (2003), Investigation of wave growth and decay in the SWAN model: Three regional-scale applications, *J. Phys. Oceanogr.*, *33*, 366–389, doi:10.1175/1520-0485(2003)033<0366:IOWGAD>2.0.CO;2.

Sanford, L. P., and J. P.-Y. Maa (2001), A unified erosion formulation for fine sediments, *Mar. Geol.*, *179*, 9–23, doi:10.1016/S0025-3227(01)00201-8.

Shchepetkin, A. F., and J. C. McWilliams (2005), The Regional Ocean Modeling System (ROMS): A split-explicit, free-surface, topography-following-coordinate oceanic model, in Ocean Modell. 9, pp. 347–404, Hooke Inst. Oxford Univ., Oxford, U.K.

Signell, R. P., S. Carniel, L. Cavaleri, J. Chiggiato, J. D. Doyle, J. Pullen, and M. Sclavo (2005), Assessment of wind quality for oceanographic modelling in semi-enclosed basins, *J. Mar. Syst.*, *53*(1–4), 217–233, doi:10.1016/j.jmarsys.2004.03.006.

Smith, J. D., and T. S. Hopkins (1972), Sediment transport on the continental shelf off of Washington and Oregon in light of recent current measurements, in *Shelf Sediment Transport: Processes and Pattern*, edited by D. J. P. Swift, D. B. Duane, and O. H. Pilkey, pp. 143–180, Van Nostrand Reinhold, Hoboken, N. J.

Sternberg, R. W., and L. H. Larsen (1976), Frequency of sediment movement on the Washington Continental Shelf: A note, *Mar. Geol.*, *21*, 36–47.

Stevens, A. W., R. A. Wheatcroft, and P. L. Wiberg (2007), Seabed properties and sediment erodibility along the western Adriatic margin, Italy, *Cont. Shelf Res.*, *27*, 400–416, doi:10.1016/j.csr.2005.09.009.

Syvitski, J. P. M., and A. J. Kettner (2007), On the flux of water and sediment into the northern Adriatic Sea, *Cont. Shelf Res.*, *27*, 296–308, doi:10.1016/j.csr.2005.08.029.

Toorman, E. A. (1999), Sedimentation and self-weight consolidation: Constitutive equations and numerical modelling, *Geotechnique*, *49*(6), 709–726.

Traykovski, P., W. R. Geyer, J. D. Irish, and J. F. Lynch (2000), The role of wave-induced density-driven fluid mud flows for cross-shelf transport on the Eel River continental shelf, *Cont. Shelf Res.*, *20*, 2113–2140, doi:10.1016/S0278-4343(00)00071-6.

Traykovski, P., P. L. Wiberg, and W. R. Geyer (2007), Observations and modeling of wave-supported sediment gravity flows on the Po prodelta and comparison to prior observations from the Eel shelf, *Cont. Shelf Res.*, *27*, 375–399, doi:10.1016/j.csr.2005.07.008.

Turchetto, M. M., A. Boldrin, L. Langone, S. Miserocchi, T. Tesi, and F. Foglini (2007), Particle transport in the Bari Canyon (southern Adriatic Sea), *Mar. Geol.*, *246*, 231–247, doi:10.1016/j.margeo.2007.02.007.

Umlauf, L., and H. Burchard (2003), A generic length-scale equation for geophysical turbulence models, *J. Mar. Res.*, *61*, 235–265, doi:10.1357/002224003322005087.

Wang, X. H., and N. Pinardi (2002), Modeling the dynamics of sediment transport and resuspension in the northern Adriatic Sea, *J. Geophys. Res.*, *107*(C12), 3225, doi:10.1029/2001JC001303.

Wang, X. H., N. Pinardi, and V. Malicic (2007), Sediment transport and resuspension due to combined motion of waves and currents in the northern Adriatic Sea during a Bora event in January, 2001, *Cont. Shelf Res.*, *27*, 613–633, doi:10.1016/j.csr.2006.10.008.

Warner, J. C., W. R. Geyer, and J. C. Lerczak (2005), Numerical modeling of an estuary: A comprehensive skill assessment, *J. Geophys. Res.*, *110*, C05001, doi:10.1029/2004JC002691.

Warner, J. C., C. Sherwood, R. P. Signell, C. K. Harris, and H. G. Arango (2008), Development of a three-dimensional, regional, coupled wave, current, and sediment-transport model, *Comput. Geosci.*, *34*, 1284–1306.

Wiberg, P. L., D. E. Drake, and D. A. Cacchione (1994), Sediment resuspension and bed armoring during high bottom stress events on the northern California inner continental shelf: Measurements and predictions, *Cont. Shelf Res.*, *14*, 1191–1219, doi:10.1016/0278-4343 (94)90034-5.

Winterwerp, J. C. (2002), On the flocculation and settling velocity of estuarine mud, *Cont. Shelf Res.*, *22*, 1339–1360, doi:10.1016/S0278-4343(02)00010-9.

Zavatarelli, M., and N. Pinardi (2003), The Adriatic Sea modelling system: A nested approach, *Ann. Geophys.*, *21*, 345–364.

A. J. Bever and C. K. Harris (corresponding author), Virginia Institute of Marine Science, P.O. Box 1346, Gloucester Point, VA 23062, USA. (ckharris@vims.edu)

C. R. Sherwood, R. P. Signell, and J. C. Warner, U.S. Geological Survey, 384 Woods Hole Road, Woods Hole, MA 02543, USA.